The Oxidation of Fe (II), Fe (II) Mineral, and Rapid Denitrification under Cyanobacterial Interfacial Competition by Novel NDFe(II)OB, *Pseudogulbenkiania ferrooxidans sp. MAI-1*

Bryce Robinson

Thesis submitted to the
Faculty of Graduate and Postdoctoral Studies
University of Ottawa
In partial fulfillment of the requirements for the
M.Sc. degree in Earth Sciences

uOttawa

L'Université canadienne
Canada's university

Abstract:

Nitrogen is an essential constituent and building unit of all living organisms, and the primary limiting nutrient on our planet such that its cycle widely depends on the diverse nitrogen-transforming microorganisms, such as denitrifiers. Oxygen minimum zones or hypoxic aquatic ecosystems account for 30-50% of all nitrogen denitrification and under dynamic transformation imbalance, of measure dependent variable modularity, little is known about discrete shifts in denitrification competition by various microorganisms of divergent metabolism; or the Fe (II) – Fe (III) redox linking process. Novel nitrate dependent Fe (II) oxidizing bacteria as rapid denitrifier and iron oxidizer can significantly oxidize various iron minerals (magnetite and ferrous mono sulfide). Evidence of nitrate dependent Fe (II) oxidation by the bacterium *P. ferrooxidans sp. MAI-1* could shed light as a novel competitor at microaerophilic (<2.0mg/L DO, -100 – +100 mV) interfacial competition with cyanobacteria *Microcystis aeruginosa* corollary to ecosystem eutrophication and concomitant microcystin production, with the goal of abating a toxic cyanobacterial bloom. Nitrate Dependent Iron Oxidizing Bacteria (NDFe(II)OB) showed rapid nitrate reduction (>25 mg/L NO2, day 7) and consequent bright-orange iron oxides. Saturation indices (day 1 and 8 SI = log (IAP/Ksp), showed non exclusive vivianite formation i.e., 3.80 and 0.44-0.55, respectively, with near complete oxidation by day 8, significantly abating logarithmic growth over a fourteen day period ($p>0.01$). N-N dichotomies are not purely exclusive, as terminal PO_4 competition differed by ~0.1 mg/L after a 15 day period, with approximately one five hundred times more N-nitrogen loss compared to P-phosphorus loss difference. Early logarithmic cyanobacteria cell counts under the presence of the competitor decreased by >20% by day 18 of growth. This is consistent with the classical view that under

primary metabolite exhaustion, interspecific competition should lead to competitive exclusion and not niche differentiation.

Résumé:

L'azote est un constituant essentiel de tous les organismes vivants et un nutriment primaire limitant sur notre planète. Son cycle est intimement relié à l'activité de plusieurs bactéries capables de transformer l'azote, comme les bactéries dénitrificatrices. Entre 30-50% de toute la dénitrification se fait dans les zones de faibles concentrations en oxygène et dans les écosystèmes hypoxiques. Le cycle de l'azote est aussi souvent relié à celui du fer. De nouvelles bactéries oxydantes du fer qui réduisent le nitrate ont été récemment impliquées dans le cycle de l'azote. La bactérie *P. ferrooxidans sp. MAI-1* est une de ces bactéries qui peut jouer un rôle compétitif dans les environments microaérophiles (<2.0mg/L d'oxygène dissout et un potential rédox entre -100 – +100 mV), tout en particulier avec les cyanobactéries *M. aerugniosa* responsables de l'eutrophisation des écosystèmes et de la production concomitante de microcystines. L'objectif de cette étude est d'étudier la compétition entre ces 2 groupes de microorganismes afin de voir si il est possible d'atténuer la prolifération des cyanobactéries toxiques. Nos résultats indiquent que les bactéries oxydantes du fer qui réduisent les nitrates (NDFe (II) OB) utilisent rapidement les nitrates (> 25 mg /L NO_2, jour 7) tout en produisant des oxydes de fer suite à l'oxydation du Fe(II). Les indices de saturation des solutions (jours 1 et 8, IS = log (IAP / Ksp), indiquent la formation non exclusive de vivianite, soit 3.80 et 0.44-0.55, respectivement, avec une oxydation presque complète au jour 8, ce qui ralentit de façon significative la croissance des bactéries sur une période de quatorze jours ($p > 0.01$). Les dichotomies N-N ne sont pas purement exclusives car la concurrence entre la PO_4 terminal diffère d'environ 0.1 mg /L après une période de 15 jours, et la perte de N-azote était environ 500 fois plus élevée que celle du phosphore. Le nombre de cellules de cyanobactéries en présence du

compétiteur a diminué de >20% au jour 18 de la croissance. Cela concorde avec l'opinion classique selon laquelle dans le cas de l'épuisement des métabolites primaires, la compétition interspécifique doit résulter de l'exclusion compétitive et non de la différenciation de niche.

.

Table of Contents:

List of Tables:

List of Figures:

Acknowledgements:

I would like to cordially thank my two supervisors Drs. Danielle Fortin and Alexandre Poulain for their intellectual and unconditional moral support throughout my creative and scientific journey. I would like to thank the following for the rational and scientific discourse and help during some aspects of the experimental process: Glenn Poirier with SEM, Jody Donnelly from Colorado U with revival protocol, Hervé Beaudoin and various members of the UOttawa Machine Shop who helped maintain the competition chamber.

List of Acronyms:

CFU	Colony Forming Units
CPCC	Canadian Phycological Culture Center
DO	Dissolved Oxygen
E_0 P	Electric Potential
EDTA	Ethylenediaminetetraacetic acid
GR	Green Rust
GR-Cl	Green Rust Chloride
GR-CO_3	Green Rust Carbonate
GR-SO_4	Green Rust Sulfate
HEPES	(4-(2-hydroxyethyl)-1-piperazineethanesulfonic acid)
KSB	Antimony potassium tartrate
MOPS	(3-(N-morpholino)propanesulfonic acid)
NAR	Membrane Bound Nitrate Reductase
NDFe(II)OB	Nitrate Dependent Ferrous Iron Oxidizing Bacteria
NEDD	N-(1-Naphthyl)ethylenediamine
NRIO	Nitrate Reducing Iron Oxidizer
NTA	Nitrilotriacetic acid
Rpm	Rotations per Minute
SD	Standard Deviation
SEM	Scanning Electron Microscopy
UV	Ultra Violet
XRD	X ray Diffraction

1. Literature Review

1.1 Project Proposal

Toxic cyanobacteria blooms such as *Microcysis aeruginosa*, have become a topic of heavy debate and great ecological concern, given their prolific behavior under anthropogenic inorganic flux. Little has been discussed in terms of effective remediation strategy of this microorganism under a source of inorganic pollution, such as when water soluble nitrogen and phosphorus are enriched. Microorganisms, such as Nitrate Dependent Iron Oxidizing Bacteria have demonstrated to rapidly denitrify fresh water ecosystems under limited oxygen environments, and could be utilized as a means of mitigation strategy through nitrogen competition (Kopf et al. 2013). We can denote competition as phosphorus assimilation and denitrification, or as non exclusive denitrification between the NDFe(II)OB and the cyanobacteria. Microbial competition between cyanobacteria and NDFe(II)OB can be achieved through the introduction of a soluble electron donor source, using a diffusion column or chamber. One side of the diffusion chamber represents the NDFe(II)OB amendment within a controlled environment, while the other side represents the cyanobacteria within a natural aquatic system. Practically speaking, a diffusion column can be added to a natural aquatic system (lake, pond etc.) to serve as a controlled environment and novel fresh water remediation strategy (Figure 1.1). The NDFe(II)OB and the ferrous iron addition that oxidizes at interface can later be disposed of as waste. Given that *Microcystis aeruginosa* are primarily nitrogen and phosphorus dependent, prefer stagnant and low oxygen waters, and are not primarily dependent on soluble carbon or Fe (II) sources, rapid denitrification by means of a competitor such as NDFe(II)OB could serve as a highly effective remediation strategy (Levy 2017). More narrowly, the addition

of soluble carbon or Fe (II) sources during early cyanobacteria growth phases, resulting in NDFe(II)OB denitrification, could diminish cyanobacterial blooms. Practically speaking, natural microaerophilic gradients that exist within aquatic ecosystems can be utilized to stimulate NDFe(II)OB denitrification, and in turn competition (Figure 1.1) (Kuypers et al. 2018). However the addition of oxygen consuming compounds such as ferrous iron, ferrous iron mineral wastes, or the use of anaerobic gas sparging are also possible mechanisms of inducing microaerophilic gradients where such microaerophilic gradients do not naturally exist.

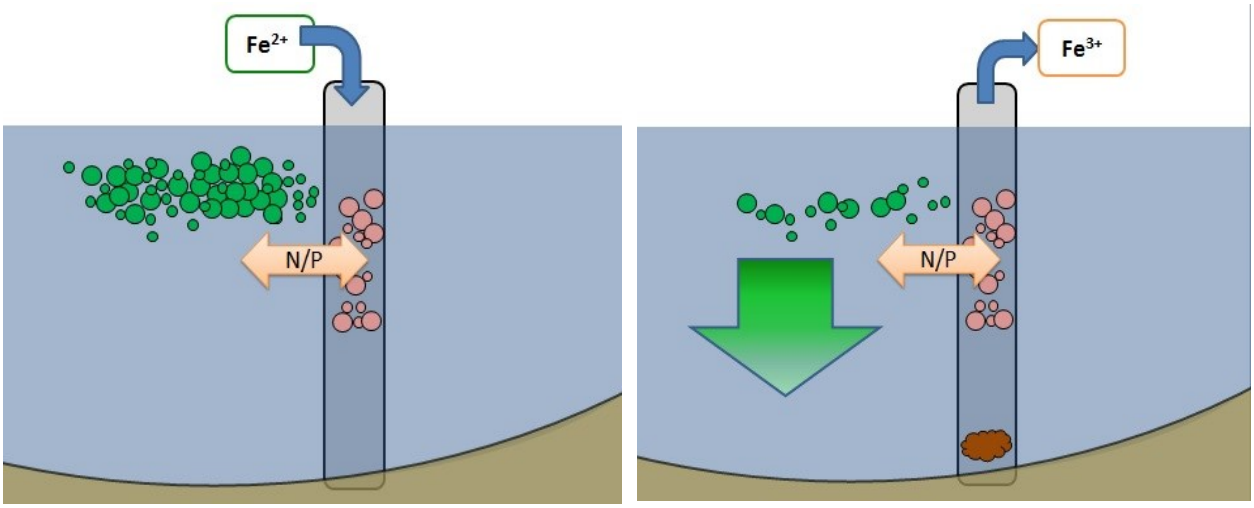

Figure 1.1 – The proposed practical application and nutrient dynamics of a diffusion chamber or diffusion column within a natural fresh water system. As NDFe(II)OB (pink) metabolizes ferrous iron, logarithmic cyanobacteria (green) cell counts decrease over time through a process known as non exclusive denitrification.Iron oxides are produced (brown) and can later be disposed as waste.

This experiment is mechanistic, where the addition of the competitor (NDFe(II)OB) during the early logoraithmic phase of cyanobacteria (day 7 of cyanobacteria growth) results in inorganic assimilation competition throughout the entirety of the cyanobacterial logarithmic growth phase (up to day 18 of cyanobacteria growth). Two separate experiments were conducted, a competition experiment with a non toxin producing cyanobacteria strain (CPCC 632) and a toxin producing cyanobacteria strain (CPCC 300). Each treatment experiment was conducted in triplicates (*M. aeruginosa* and *P. ferrooxidans* together in the chamber), along with a triplicate of control experiments (*M. aeruginosa* alone in the chamber). The experiment was designed in order to obtain a difference of logarithmic cyanobacteria cell counts and primary metabolite assimilation between exclusive cyanobacteria, and cyanobacteria with an added competitior (*P. ferrooxidans*). Ferrous iron additions opposite to the cyanobacteria side were consistent throughout both the control and treatment experiments. The consistent ferrous iron addition procedure was neccesary to avoid the argument that a decreased cyanobacteria logarithmic cell counts may have been attributed to phosphorus ferric iron sorption in the treatmentand and not due to competitor assimilation. In the experimental treatment, the cyanobacteria was introduced to one side of the diffusion chamber and the competitor NDFe(II)OB was introduced to the other side of the diffusion chamber allowing for basic media diffusion between the two species.

1.2 Objectives and Hypotheses

The objective of the experiment is to utilize rapid denitrifying microorganism *P. ferrooxidans* to compete with non exclusive nitrogen species, specifically nitrate and nitrite, in

attempt to abate a cyanotoxic bloom of *M. aeruginosa* of both toxin and non toxin producing strains. Given that *M. aeruginosa* cyanobacteria blooms are primarily dependent on the concentration and presence of inorganics such as phosphorus and nitrogen, I can predict that competition by means of non exclusive denitrification will reduce the size (cell counts) and longevity of a bloom (Ernst et al. 2005; Levy 2017). Under low phosphate concentrations (> 0.1 mg/L, <1 mg/L) we can predict that the cyanobacteria will become more dependent on nitrate in terms of bloom size (cell counts) and longevity (Ernst et al. 2005). This competition objective is conducted with the intention of remediating cyanobacteria dominated fresh waters under logarithmic growth, by means of non exlusive denitrification through the introduction of a novel competitor. This study was completed to determine whether the introduction of the competing bacteria *P. ferrooxidans* would result in the competitive exclusion of *M. aeruginosa* when producing an early bloom. Hypothesis: *M. aeruginosa* have been detailed to exist within many fresh water communities, however little is known of cyanobacteria growth mechanisms when existing with other organisms that share similar niche. Little is known of how cyanobacteria mechanistically interact and compete with other organisms that share similar nitrogen pathways under logoarthmic growth periods. Such competing organisms include denitrifying microorganisms such as NDFe(II)OB (Newton et al. 2011; Kuypers et al. 2018). (1) The addition of *P. ferrooxidans* at the early logarithmic growth phase of the cyanobacteria (day 7) will result in mechanistic non exclusive nitrogen competition by means of *P. ferrooxidans* denitrification, towards both *M. aeruginosa* strains (non toxin and toxin). (2) During the competition period or after day 7 of cyanobacteria growth, *P. ferrooxidans* will begin to rapidly denitrify nitrate to nitrite, and will terminate with a nitrogen:phosphorus assimilation molar ratio exceeding 4:1 at day 15. (3) Rapid denitrification of total nitrogen species by *P. ferrooxidans* will result in rapid

nitrogen loss (> 4:1 N:P assimilation) by day 15, and in turn this inorganic concentration disparity will result in an early cell death phase (a signficant drop in cyanobacterial cell counts) of both the cyanobacteria strains. In effect, total non exclusive nitrogen loss by means of the competitor *P. ferrooxidans* will result in a diminished cyanobacteria logarithmic growth phase (a total cell count reduction of ~25% by day 18) when compared to the control logarithmic growth phase (cyanobacteria without the competitor). In summary, logarithmic cell counts of the cyanobacteria in the treatment experiment will significantly reduce compared to the control experiment, as a product of total denitrification by the competitor.

1.3 The Nitrogen Cycle

Nitrogen is an essential constituent and building unit of all living organisms and the primary limiting nutrient on our planet. Its cycle widely depends on the diverse nitrogen-transforming microorganisms (Kuypers et al. 2018). The atmosphere is almost 80% N_2, but not accessible in this form, and can enter ecosystems via two routes, the relative importance of which varies, by atmospheric deposition in wetfall such as rain, snow, cloud, fog or particulates; while the other is via nitrogen fixation (Smith et al. 2012; Vitousek and Howarth, 1991). Chiefly, atmospheric nitrogen exists as the largest free source of nitrogen, excluding unfree demarcated ammonia, confined to various unidentified rocks and biologically inaccessible sediments, and is utilized by a wide variety of different microorganisms (Kuypers et al. 2018; Stein and Klotz, 2016). Traditionally, nitrogen transformation has been expressed as one balanced cycle; however it is more accurate to express the overarching cycle as six similar but distinct fluxes with different measures and magnitudes: assimilation, ammonification, nitrification, denitrification,

anaerobic ammonium oxidation (anammox) and nitrogen fixation, which alter the oxidation state of nitrogen to toxic and non-toxic forms (Kuypers et al. 2018; Fang 2004). Transformation of bioavailable dinitrogen gas is ensued by a few but diverse nitrogen fixing bacteria and archaea communities, through a process known as nitrogen fixation. Current estimates detail microbial total nitrogen fixation (~425 Tg nitrogen yr−1) as an exceedance or parity to the productivity of atmospheric gas by denitrification and annamox processes (~350 Tg nitrogen yr−1) by approximately twenty percent (Gruber 2008; Gruber and Galloway, 2008). Anthropogenic activity has dramatically marked the departure of historic nitrogen transforming cycles, chiefly the global total bioavailable nitrogen, corollary to agricultural fertilizers, population growth and food and waste production (Erisman 2008; Galloway 2008). Bioavailable redox-reactive nitrogen species are rare to many environments and are intermediates whom measures are governed by microbial activity that alter the oxidation states, namely but not only, nitrification and denitrification (Kuypers et al. 2018). Denitrification is the operation wherein high oxidized potentials of nitrogen are transformed to high reduction potentials, through processes of dissimilatory and assimilatory reduction (Moreno-Vivian et al. 1999; Zumft 1997). Processes such as these, are mediated by several distinct nitrogen transforming enzymes with bound intermediate incorporated enzymes of distinct redox states like NAR for example, such that many of which have not yet been fully detailed or identified (Moreno-Vivian et al. 1999).

Nitrogen is also a requirement for essential biosynthesis of key cellular components, principally proteins and nucleic acids. Specialized nitrogen reducers or oxidizers are also known to incompletely cycle nitrogen potentials as they contain a lack of genes permitting at most the organism to, carry out one or few of the transformations (Preisler et al. 2007). Naturally

occurring, unfavorable growth conditions engender recycling communities that foster commensalism and mutualism, such that nitrogen-transforming bacteria have demonstrated immense versatility in function, rendering the classification as traditional denitrifiers to nitrifiers as nonstandard nomenclature and realize organized niches that are concordant to their biochemical to biogeochemical fitness (equations 1&2). Four main biochemical reactions exist, viz. (1) atmospheric dinitrogen fixation accessible by members that carry the nitrogenase metalloenzymes (Eady 1996), (2) ammonia oxidation to, but not exclusively terminal nitrate by a series of oxygenases and oxireductases (Hooper et al. 1997), (3) nitrate reduction to, but not exclusively as terminal dinitrogen gas, by a series of reductases (Saraiva et al. 2004; Moreno-Vivian et al. 1999) and, (4) the transformation of nitric oxide to hydroxylamine and terminal hydrazine, the most potent nitrogen reductant in nature, by comproportionation of ammonia (Caranto and Lancaster, 2017); with the fourth operation being the most obscure. Formulaic systems rely on nitrification (ammonium to nitrate) vis-à-vis denitrification (nitrate to dinitrogen gas and/or ammonia) to make clear of, but at cursory glance, the nitrogen cycle (Robertson et al. 2016).

(1) Nitrification: NH_3 (g) → N_2 (g) → N_2O (g) → NO (g) → NO_2^- (aq) → NO_3^- (aq)

(2) Denitrification: NO_3^- (aq) → NO_2^- (aq) → NO (g) → N_2O (g)

Pollution and contamination in the form of nitrogen, most notably man-made agricultural fields, and ancillary types such as mine waste systems, have strongly transformed microbial network systems substantially by nitrogen accumulation in the form of sinks (Galloway 2008). Such sink/source transformations result in discrete shifts in both, substrate competition and/or

cooperative interactions, of measure dependent variable modularity; which is most notable of organismal communities of highly different metabolisms (Kuypers et al. 2018). However, global scale biosphere nitrogen balances can be largely characterized as nitrogen homeostatic, owing to extensive recycling. Competing bacteria of similar nitrogen niche cannot however, always be described unambiguously as nitrogen competing, as many microorganisms that utilize the same pathways of nitrogen will also utilize other restraining substrates and compete amongst other factors, such as signalling ligands (though largely autonomous in prokaryotes) as well as toxin production (Lam and Kupyers, 2011). Therefore, these models cannot be represented solely as nitrogen-nitrogen dichotomies and have been shown to respond to environmental perturbations outside conformity to traditional boundaries, such that little is known about community discrete changes, community unique pathways, the degrees of interactions and varying microbial nitrogen transforming reactions (Kuypers et al. 2018).

Within ocean gyres and recently, fresh water ecosystems, the main transforming processes are nitrogen assimilation and amongst many species, nitrogen fixation, by means of various species of dominant cyanobacteria (dually heterocyst and non-heterocyst) communities, as the primary supply of newly bioavailable nitrogen; owing to the vast aquatic area the bacteria may occur (Berman-Frank et al. 2003). Oxygen minimum zones or aquatic hypoxia ecosystems account for 30-50% of all aquatic nitrogen denitrification and under dynamic transformation imbalance, waste water treatment is applied, but little is known about denitrification competition by various microorganisms of divergent metabolism under rich, eutrophic conditions (Lam and Kuypers, 2011; Lam et al. 2009). Freshwater aquatic eutrophication, owing to nitrogen and pragmatic combinations of phosphorus and others, is one of the main and growing contemporary

ecological concerns worldwide, such that increasing anthropogenic activity, inorganic flux imbalances and water quality deterioration evolve as multifactorial dilemmas. Understanding the mechanisms, sources and drivers of eutrophication altering ecological processes will therefore aim to benefit mitigation strategies of the future (Rabalais, 2001; Mitsch et al. 2005).

Nitrogen redox reactive intermediaries are described and characterized with individual solubility and volatization constants such that echelon dependent gas transfers at water surface will occur (Donelon et al. 2002; Strumm and Morgan, 1996) (equations 3&4). Henry's law constants, also known as solubility, of trace gases are of environmental importance such that the degree or measure of aqueous-phase and gas-phase concentrations can be determined when delineating atmospheric chemistry and aqueous to gas and vice versa cycling. There are several ways of detailing the solubility of a gas in a water system, chiefly Henry's law constant is defined as:

$$(3)\ k_H \triangleq c_a/p_g$$

where, ca is the concentration of the species within aqueous phase and pg is the partial pressure of that species in gas phase. If k_H refers to standard conditions, that is $T^\theta = 298.15$ K, is will be denoted as k_H^θ. Henry's law constant can also be expressed as the dimensionless ratio between the aqueous and gas phase concentration, by the algebraic inclusion of the ideal gas law:

$$(4)\ c_a/c_g = k_H \times RT$$

where, R is defined as the gas constant (8.314 J/molK) and T denotes temperature in Kelvin. Knowing the solubility of the aqueous phase by experimental quantification, one can determine the amount of gas phase present at denoted time (c_g). Using geochemical equations, nitrogen reactive species can be determined and volatile intermediaries (NO, N_2O, N_2) cannot solubilize at water interfaces by means of atmosphere, at atmospheric pressure and under natural atmospheric concentrations in the form of sufficient and accessible solubility (Donelan et al. 2002); unless as dissolved, or catalyzed to a more soluble state by means of a microbial, enzymatic process (Kuypers et al. 2018).

1.4 The Phosphorus Cycle

As an element with a true sedimentary cycle, only minimal measures of phosphorus is found occurring in the atmosphere (Smith et al. 2012). The P cycle largely occurs in aquatic systems moving from land to sea by means of chiefly fresh water transport and thus hyper stimulate bacterial logarithmic growth like cyanobacteria, by rich runoff or deposition (Smith et al. 2012). Most of the phosphorus that exists is trapped within sediments and rock reservoirs such as apatite, and is released naturally by weathering, erosion or biotic leaching but can be released in excess by anthropogenic activity namely, agricultural and mining runoff (Smith et al. 2012). The major bioavailable forms are inorganic anions, PO_4^{3-} and HPO_4^{2-} and they repulse many negatively charged compounds in soils and clays, allowing for simple transport to moving aquatic systems and consequently transform into three main states (1) particulate organic, (2) dissolved organically bound phosphates, and (3) inorganic phosphates (Smith et al. 2012). In ocean systems, largely organic phosphates are taken up by phytoplankton, detritus feeders and

zooplankton and thus excreted as inorganic and the remainder largely assimilated by bacteria (Smith et al. 2012). Here, unconsumed or untransformed phosphorus is buried into shallow fresh and deep ocean deadlocked sediments, naturally depleting the mid to surface open water systems, unaffected by rich nutrient upwelling, pollution or heavy planktonic assimilation (Smith et al. 2012). Microcystis species of cyanobacteria have demonstrated the ability to outcompete many planktonic species, given their immunity to predation by many planktonic crustaceans (primary predation) and many other introduced types, namely the zebra mussel, as many concomitant chemicals and toxins have been shown to inhibit planktonic crustacean growth by protease inhibition (Michalak et al. 2013; Harke et al. 2016; Steffen et al. 2013). Some species of *Microcystis* have developed a unique scavenging mechanism, whereby gas vesicles inflate, enabling them to rise to surface waters where runoff flux may be elevated, or in the case of deflation, enabling them to sink to bottom sediments when phosphate in open water systems are lower (Walsby et al. 2007). Some microorganisms such as cyanobacteria are known to internalize phosphate with transport system component Pst namely, PstB1, strictly conditional on low to limited levels of phosphorus accessible in the immediate environment and not enriched eutrophic water systems (Hudek et al. 2016); *Microcystis sp.* however, are not known to internalize phosphate, but can even so internalize nitrite if found in rich conditions within the proximal environment (Chen et al. 2012). Recent research has moved away from phosphate, as studies have demonstrated measure dependent toxin production corollary to increased levels of nitrogen species, as nitrogen is a primary building block of amino acids and peptides (Gobler et al. 2016). Practically speaking, singly phosphate reduction will not reduce the degree of toxin produced. It may be that our attention to phosphate is too strict, and a broader more pragmatic application reducing or limiting inorganic nutrients of non-point source pollution, dually N and

P, as the addition of soluble carbon shows no effect on cyanobacterial growth or toxic blooming (Levi, 2017; Chaffin et al. 2013).

1.5 The Iron Cycle

Iron is the fourth most abundant element within the earth's crust and serves as, after oxygen, one of the most abundant primary life sustaining redox reactions for the microbial world, and can form stable compounds within the ferrous divalent and ferric trivalent state (Emerson et al. 2010). The Fe (II) – Fe (III) redox is also an important redox couple in natural environments, and can be mediated by few but vastly different types of biological agents, ranging to environments that is growth limiting such as the case for much oceanic algae (Morissey and Bowler, 2012), or in iron rich sediments and within the earth's enriched crust (Emerson et al. 2010). Moreover, at oceanic hydrothermal vents, iron is not a limiting nutrient, and is overwhelmingly the case for many oxic-anoxic interfacial habitats occupied by a diverse range of lithotrophic microorganisms (Emerson and Weiss, 1999; Dodd et al. 2007). In coastal ocean surfaces to sediment, iron is in an enriched source provided by input from rivers, lakes and bioturbation mixing (Emerson and Weiss, 1999). The open oceans however, obtain most of its iron from continental Aeolian dust blow off and volcanic discharge and are the most anemic waters of the world (Moore and Braucher, 2008), whereas deep ocean hydrothermal vents supply diverse microbial communities with most of the iron under deeper anoxia, growing primarily under colder conditions (<100°C) compared to black smokers (<300°C) (Raiswell and Canfield, 2012; Canfield and Thamdrup, 2005; Emerson and Moyer, 2010). The acidity of various environments also plays a significant role on the redox potential of iron corollary to the

microbial communities that utilize it, such that both ferrous and ferric iron can be utilized in the form of energy; for example acid mine drainage systems will helm more stable iron and highly oxygenated zones of neutral waters will become less stable, given its energetic favourability to oxidation (Straub et al. 2001). At neutral pH, the role and mechanisms involved in electron transfer to and for iron minerals are still very poorly understood. Primarily in the form of Fe-oxides, iron reducing to oxidizing communities composed of various archaea and bacteria communities can utilize the ferric iron potential both aerobic and anaerobic respiration, and under anoxia by means of anaerobic dissimilatory ferric iron-reducing and ferrous iron-oxidizing bacteria (Straub et al. 2001). This has been established as an important pathway for carbon metabolism and other transformations (Straub et al. 2001). The Fe (II) – Fe (III) redox cycle is a remarkably complex process, and influenced by a wide variety of different chemical conditions and environments such as the vastly different nitrogen fluxes, which links iron to many unique but related biogeochemical processes across the globe (Straub et al. 2004).

Sixteen iron hydroxides or oxide hydroxides exist, and may helm organic and inorganic constituents termed collectively as, iron oxides (Weber et al. 2006). Aquatic sediments and wetland soils can contain up to several mmol of iron oxides per kg of dry matter (Lovley et al. 1996). Iron oxides are dominant electron acceptor in such environments, however, in oceanic water sediments sulfate serves as the prominent electron acceptor due to its abundance over iron (Lovley et al. 1996). Anaerobic oxidation by microorganisms however, has only been discovered recently, with most notable phototrophic purple non-sulfur bacteria (Widdel et al. 1993), or nitrate dependent iron oxidizers, whereby the ferrous to ferric potential is utilized in the form of energy under anaerobic to microaerophilic environments (though largely restricted to deep or

anoxic waters where chemical oxidation does not restrict development (Emerson et al. 2010; Pérez-Guzmán et al. 2010), as studies have shown that iron could also be oxidized by bacteria with molecular oxygen. At circumneutral pH, nitrate and its intermediate or reduced derivatives have a much higher positive reduction pathways compared to the iron redox pair (E_0 P values: NO_3/NO_2, +430 mV ; NO_2/NO, +350 mV ; NO/N_2O, +1180 mV ; N_2O/N_2, +1350 mV), and therefore serve as an excellent electron acceptor for nitrate reducing iron oxidizing microorganisms (NRIOs) from ferrous oxidation (Straub et al. 1996; Weber et al. 2006). That is to say, NRIOs have shown to play an important role in the formation of iron oxides under both aerobic and anaerobic environments, and little is known regarding the degree to which the iron-oxide forming pathways vary.

1.6 Iron Minerology and Green Rusts

NRIOs are known to be producers of various iron hydroxides and oxyhydroxides (collectively termed iron oxides or Fe (III) oxides), which are ubiquitous in the pedosphere and originate from the aerobic weathering largely ferromagnesium and iron sulfide minerals (Cornell and Schwertmann 1996). The transformation depends on factors such as pH, redox potential, temperature, degree of hydration or dehydration, the rate of oxidation or reduction and biotic mineral transforming activity (Cornell and Schwertmann 1996). Iron oxides are known to serve as redox buffers in soils and sediments including water interfaces, and are also known to aggregate with both organic and inorganic particles (Straub et al. 2004). They can sorb anions and cations, which in turn impact the movement of nutrients in aquatic and soil systems (Straub et al. 2004). A number of Fe bearing minerals can exist within aquatic sediments produced by

NRIOs, such as transitional green rust (GR) (layered Fe (II) – Fe (III) oxyhydroxides), poorly crystalized ferrihydrite, vivianite to poorly crystallized vivianite (Straub et al. 2004) (equations 5,6 &7). Green rusts are known to serve as transitional metastable intermediaries to many iron oxides at circumneutral pH and higher (i.e. 7-9) within aquatic ecosystems (Cornell and Schwertmann,1996; Ilberta and Bonnefoy, 2013). The general formula of green rust exists as $[Fe^{2+}_{(6-x)}\ Fe^{3+}_{x}\ (OH)_{12}]_{x}+ [(A)_{x/n}\cdot yH_2O]^{x-}$ whereby A represents an anion bearing a non-valent electron, namely CO_3^{2-}, Cl^- (rhombohedral), or SO_4^{2-} (hexagonal) while other varieties have reported less common anions such as NO_3^- for instance. Some examples are below (Mendiboure & Schöllhorn, 1986):

(5) Carbonate Green Rust: GR (CO^{2-}_3): $[Fe^{2+}_4Fe^{3+}_2(HO^-)_{12}]^{2+} \cdot [CO^{2-}_3\cdot 2H_2O]^{2-}$

(6) Chlorine Green Rust: GR (Cl^-): $[Fe^{2+}_3Fe^{3+}\ (HO^-)_8]^+ \cdot [Cl^-\cdot nH_2O]^-$

(7) Sulfate Green Rust: GR (SO^{2-}_4): $[Fe^{2+}_4Fe^{3+}_2(HO^-)_{12}]^{2+} \cdot [SO^{2-}_4\cdot 2H_2O]^{2-}$

The type of green rust forming is highly dependent on the saturation and nature of the water system solution, such that the degree or concentration of particular anions will influence a certain type. Anions with smaller radii are bound more strongly, for example high sulfate concentrations may promote sulfate green rust formation, but phosphate for example in low to moderate concentrations has been shown to inhibit or restrict to a degree (chiefly dependent on saturation indices), the formation of some types of green rusts and promotes the direct transformation to vivianite, equally so in the event of a limited phosphate presence (Nriagu and Dell, 1974). Vivianite produced by particular NRIOs namely BoFeN1, under the presence of enriched nitrite and ferrous iron has been shown to transform to a poorly crystalline geometric

phase, with increased crystallite size over 72 hour periods of enriched nitrate-nitrite (aq) and Fe^{2+} (aq) exposure time, qualitatively transforming from white to yellow-green and terminal bright orange phase quantitatively to a BoFeN1 unique $[NO_3^-]_x$ – vivianite intermediary phase (Miot et al. 2009). GRs altogether, are vital intermediate phases which are largely produced due to partial oxidation of zero valent iron, Fe (II) to Fe (III) by means of iron oxidizing microorganisms under anoxic systems or through microaerophilic waters and oxic – anoxic interfaces, or by partial reduction of Fe (III) - oxides to Fe (II); contingent on circumneutral waters. Vivianite authigenesis moreover, is an important mineral associated with lacustrine sediments that results in phosphorus burial in the form of a sink, and its formation is vital in the restoration of eutrophied lakes, including induced P precipitation and thus burial, by iron deposition to anemic lake systems (Rothe et al. 2016).

1.7 Microorganisms: Cyanobacteria & Nitrate Reducing Iron Oxidizers

1.7.1 Microcystis aeruginosa

Cyanobacteria are photosynthetic, morphologically diverse ancient aquatic organisms and co-exist in communities under different forms ranging from unicellular, filamentous to non-filamentous, and planktonic to benthic ecosystem communities (Levy 2017). Cyanobacteria have demonstrated a capacity for a large plethora of metabolic potential and are well known for their ability to change markedly thereof, such as denitrification, nitrogen fixation (primarily owing to specialized filamentous cells), to a dramatic departure of sulfide dependent anoxygenic photosynthesis (Kuypers et al. 2018; Shindler et al. 2008). *M. aeruginosa* are highly prolific in fresh water ecosystems of moderate to tropical climates, to the extent that they are a common

cyanobacteria strain, and popularized by the recent, dramatic lake Erie cyanobacterial blooms of the great lakes region, North America (Levy 2017; Henry 2014; Watson et al. 2016). *Microcystis aeruginosa* and non-heterocyst slow growing cyanobacteria and photoautotrophs, are non-filamentous, ammonia assimilating and nitrogen denitrifying bacteria (high affinity to: NH_4^+, NO_3^-) (Schindler et al. 2008) (Figure 1.2). The toxin producing strain (CPCC 300) is capable of generating 204 ug/kg dry weight microcystin, a heptapeptide toxin. Shifts in strategy to abate toxic bloom production has ranged from the creation of artificial wetlands to capture inorganic runoff, to the reduction in both P and N pollution and silicate flocculation (though this largely eutrophies water bodies and increases benthic zone maturation rate, and may likely as well affect healthful planktonic development by co-flocculation) (Paerl et al. 2016; Levy 2017). Nonetheless, all such large strategies are highly dependent on public awareness. Even so, very little has been proposed regarding interspecific competition of other organisms of similar niche or pathway.

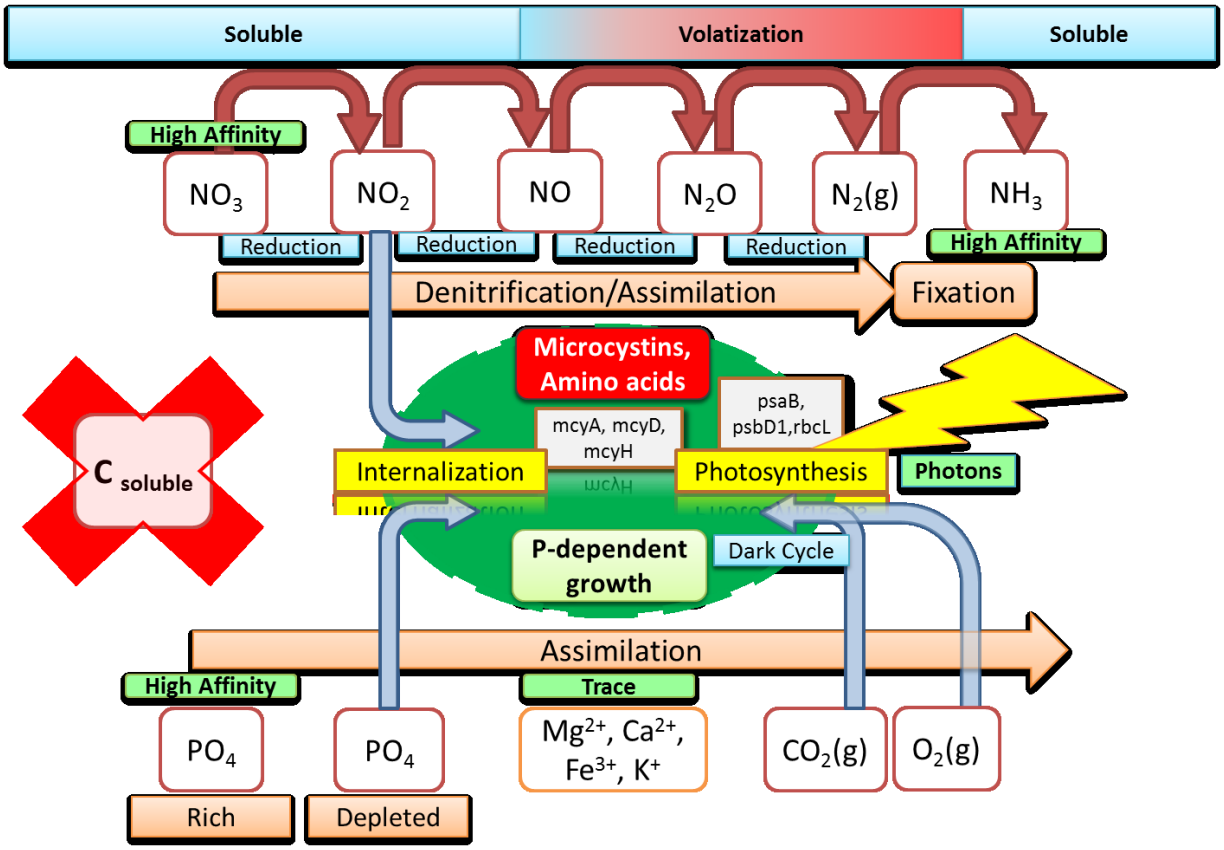

Figure 1.2 – Cyanobacteria mechanics and chemical metabolism, representing the light cycle, dark cycle, assimilation and internalization. Non-heterocyst organisms such as *M. aeruginosa* cannot fixate dinitrogen gas to ammonia or internalize phosphate.

1.7.2 Microcystin Toxicology

Cyanotoxic blooms are usually found with concomitant toxin production with primary target organs in mammals, such as the common microcystin-LR. However the microcystins produced can vary from organism to organism ranging from amino acids (neurotoxic), polyketides (dermatoxic), alkaloids (hepatotoxic, neurotoxic) and cyclic peptides (chiefly hepatotoxic), with cyclic peptides including both microcystin and nodularin types (Dawson 1998). Microcystins have also been shown to inhibit phosphatase enzymes common to *E. coli* and human kidney cells of humans and others (Levy 2017). Drinking and inhalation, particularly

under the case of heavy rolling tide aerosolization, whereby agitation of surface waters creates localized inputs of microcystins into the air, may cause fatal poisonings, paralysis and liver failure (Cheng et al. 2007).

1.7.3 Novel NDFe(II)OB P. ferrooxidans sp. MAI-1

The Fe(II)/Fe(III) redox couple is an important electron supplant for energy in natural environments and is largely mediated by microorganisms under stable oxygen free waters, where the first iron-oxidizing nitrate-reducing bacterium was discovered by Straub et al. 1996. In traditional denitrification, a carbon source acts as an electron donor, however in the case of NRIOs namely, *Pseudogulbenkiania ferrooxidans sp. MAI-1*, a fast growing iron oxidizing, nitrate dependent chemolithotroph isolated from the iron rich lake of Lake Matano of Indonesia, utilizes iron as the electron donor, and the biogeochemical processes involved under microaerophilic to anaerobic conditions are largely overlooked (Kopf et al. 2013). Oxygen deprived waters create a unique ecosystem in which future research is warranted for the amelioration of various unknown foundational to chemical processes, involved in chemical interactions with minerals and other competing microbes, including a better comprehension of nitrogen and iron biogeochemical cycling. Many studies have demonstrated that rapid Fe(II) oxidation by means of accelerated denitrification to reactive nitrogen derivatives (as well as reactive nitrate, though typically stimulated by mineral catalysis) yields unique to specific iron-oxide junctures such as green rust, iron oxyhydroxides, siderite and vivianite (Kopf et al. 2013). Recently it has been shown that the introduction of carrying chelating agents such as NTA, EDTA, citrate (with citrate being to most relevant to natural systems) leads to a more rapid rate

of iron oxidation by assimilation, and in inorganic environments are likely to highly contribute to iron cycling, including the immobilization of contaminants on iron oxyhydroxide surfaces (Straub et al. 2004). Four pathways exist in which *P. ferrooxidans* can oxidize iron along with concomitant mineral formation: (1) mineral catalysis through biotic generated positive redox potentials, (2) cell surface catalysis, (3) ligand catalysis by means of a chelator or carrier agent namely citrate, EDTA, NTA and others, (4) and enzymatic catalysis commonly nitrate reductases (Maalcke et al. 2014). However based on the proteomics of *P. ferrooxidans MAI-1*, structure and function are largely unknown (Kopf et al. 2013, Figure 1.3). Being able to distinguish the mechanism and turnover rates of iron oxidation and nitrate denitrification is vital in determining the mechanisms involved in bio-corrosion and bioleaching, especially carrier electro-winning prototyping (Schippers and Sand, 1999). Altogether, most probable number counts have shown that NRIOs make up ~1.0 percent of nitrate reducing communities but it does not demonstrate the magnitude or degree of metabolic activity or total contribution to the nitrogen cycle and electron transfer flow under anaerobic to microaerophilic conditions (Kuypers et al. 2018).

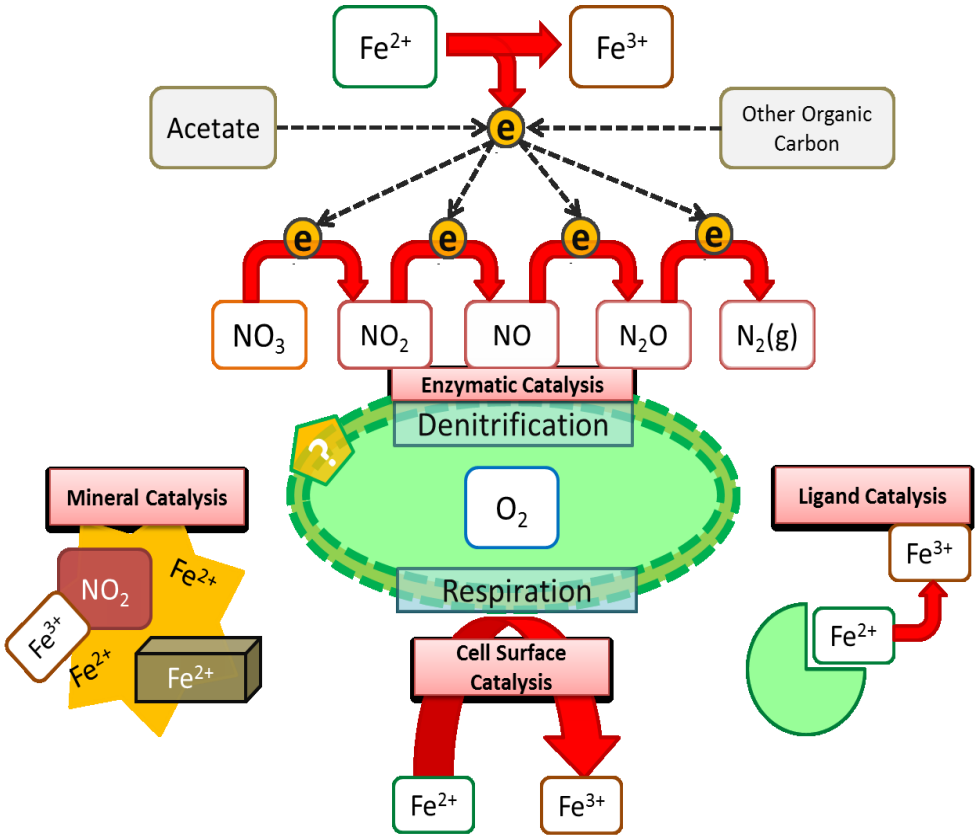

Figure 1.3 - The mechanics and chemical metabolism of *P. ferrooxidans MA1-I*, modified from Kopf et al. 2013.

2 Methods

2.1 Strains & Growth Adaptation Experiments

P. ferrooxidans arrived in 10% w/v sucrose, LB in vacuum dried atmosphere flushed with filtered nitrogen gas obtained from the University of Colorado (S. Kopf). Revival through respiration was performed under lysogeny broth; 1.5 g/100 mL sterilized media at 30°C in the presence of aerobic atmosphere, and was maintained and purified using nutrient agar plates. Acclimation of the bacteria to acetate from peptone sugar was performed by gradual serial dilutions of peptone with 100% base media as acetate (10 mM) (with 100 mg / L PO_4 enriched to

encourage healthy growth) as the desired carbon source. Base media was maintained throughout the duration of the acclimation procedure and the sugar was gradually weaned after a period of >30 days to instigate a shift of carbon source metabolism by transferring 4 mL of mid to late exponential phase growth to a more diluted media, and monitored using spectrophotometric optical density 600 nm (100%, 90.0%, 75.0%, 50.0%, 25.0%, 12.5%, 6.25%, 3.00%, 1.00%, 0.50%, 0.01%, 0.00%). *Microcystis aeruginosa* strains were obtained from the Waterloo Culture Center, CPCC 300 (toxin) isolated from Pretzlaff pond Alberta and 632 (non-toxin), isolated from Lake Mendota Wyoming. Both cyanobacteria strains were received in a liquid, modified BG-11 culture.

2.2 Competition Experiment Setup & Experimental Media

2.2.1 Modified BG-11 Denitrifying Media

Cyanobacterial strains were maintained in modified BG-11, prepared using 0.509 g/L sodium nitrate, 4.77 mg/L potassium monobasic phosphate, 0.075 g/L magnesium sulfate heptahydrate, 0.036 g/L calcium chloride dehydrate, 0.006 g/L citric acid, 0.006 g/L ferric citrate, 0.001 g/L nitrilotriacetic acid, 0.020 g/L sodium carbonate, and 2.5 g/L HEPES buffer. A 1000x trace metals solution was prepared using the modified Wolfe's Mineral recipe, i.e., 0.012 g/L nitriloacetic acid, 0.5 g/L $MnSO_4 \cdot H_2O$, 0.1 g/L $CoCl \cdot 6H_2O$, 0.1 g/L $FeSO_4 \cdot 7H_2O$, 0.1 g/L $ZnSO_4 \cdot 7H_2O$, 0.001 g/L $CuSO_4 \cdot 5H_2O$, 0.01 g/L H_3BO_3, 0.01 g/L $Na_2MoO_4 \cdot 2H_2O$, and 0.01 g/L $NiCl_2 \cdot H_2O$. A 100x vitamin solution mix was prepared using the modified Wolfe's vitamin recipe, whereby final growth media composition per litre included 10 mg pyroxidine·HCl, 5.0 mg thiamine·HCl, 5.0 mg riboflavin, 5.0 mg nicotinic acid, 5.0 mg calcium pantothenate, 5.0 mg

p-amino benzoic acid, 5.0 mg thioctic acid, 2.0 mg biotin, 2.0 mg folic acid, and 100.0 ug cyanocobalamin.

2.2.2 Modified Denitrifying Media

The growth maintenance medium for *P. ferrooxidans* was modified from Kopf et al. 2013, after revival by (LB) lysogeny broth, which contained 0.4698 g/L magnesium sulfate heptahydrate, 0.099 g/L calcium chloride dehydrate, 0.3 g/L ammonium chloride, 0.8444 g/L sodium nitrate, 4.185 g/L MOPS buffer, 1.3608 g/L trisodium acetate and rich 0.1 g/L potassium monobasic phosphate to encourage growth during acclimation. *P. ferrooxidans* was grown during maintenance with a 1000x trace metals solution which was prepared using modified Wolfe's Mineral solution, as described before. The same 100x vitamin solution mix was prepared using the modified Wolfe's vitamin as described before, in section 2.2.1

2.2.3 Competition Media

Experimental media for the diffusion chamber competition (i.e. the modified denitrifying media) contained a total 4.5 mM nitrate sodium nitrate, 2.5 g/L HEPES buffer, 1.11 mg/L PO_4, 0.6805 g/L trisodium acetate, 0.2724 g/L magnesium sulfate heptahydrate, 0.15 g/L ammonium chloride, 0.068 g/L calcium chloride dehydrate, 1 mL modified Wolfe's Mineral per litre, as described before, and 1 mM ferrous iron from anaerobic ferrous chloride x100 stock, introduced to the anoxic (Ar) media using a pre-flushed syringe (N_2). In order to simulate environmentally relevant conditions, no vitamins were introduced to the experimental media. All media were

adjusted to a final pH of 6.9-7.0 using 1 mM KOH or 1 mM HCl, created under atmospheric conditions at 25°C and sterilized using 0.2 micron vacuum or syringe microfiltration in pre-autoclaved (121°C >15 psi 20 minutes) glassware. Sterilization of the diffusion chamber was performed under UV light for a 24 hour period. All bacterial and media benchtop transfers were performed under a 15 cm radius of Bunsen burner. Sterilization of vitamin and or trace metal mineral mix was always performed using filter sterilization to prevent the heat/pressure oxidation of metals in solution.

2.3 Designing the Competition Chamber

The chamber experiment consisted of a control group and treatment group. The control group represents *M. aeruginosa* on one single side over an eighteen day growth period with a 1 mM ferrous iron addition on the opposite side of the chamber. The treatment group represents both *M. aeruginosa* and *P. ferrooxidans* together on separate sides, with a 1 mM ferrous iron addition on the *P. ferrooxidans* side. In summary, the treatment represents a competing community for over a eighteen day growth period. The expression denoted as total average, represents the average concentration of the entire system, or the average concentration of the two distinct and separate chamber sides combined. The expression total average, is necessary to resolve the discrepancy in concentrations of each side. One 5 cm and one 6 cm plastic gasket were used to prevent medium leakage, 0.2 um replaceable Millipore filters to prevent bacterial diffusion and cross over, and eight 3 cm long screws to hold the growth containers together separated by Millipore filter paper. Simple osmosis was carried out with constant medium

turbation by aerobic (atmosphere 1.0 psi, 6.0-9.0 mg/L DO) and anaerobic (99% purity argon 1.0 psi, 1.3-1.6 mg/L DO) gaseous influx to simulate a microaerophilic interface.

a) b) c)

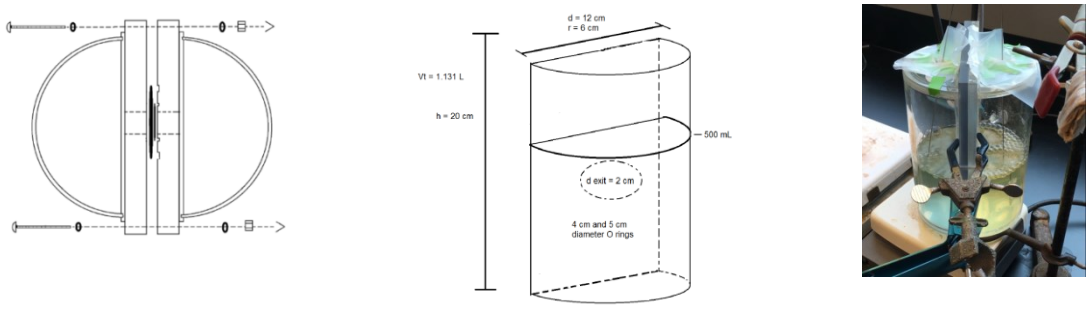

Figure 2.1 – Diffusion competition chamber design, whereby nutrients and dissolved gases are transferred between microcosms by simple diffusion and gaseous turbation; a) above partial view, b) cut plane partial view, c) designed and functioning model.

2.4 Quantification of Cell Growth and Counts

Cyanobacterial cell counts were quantified using modified BG-11 nutrient agar growth plates containing (w/v) containing 0.5% agarose gel, 0.5% peptone, 0.3% yeast extract, 0.5% sodium chloride prepared in one litre ultrapure deionized water, along with 1 mM nitrate, 10 uM phosphate, 0.075 g/L magnesium sulfate heptahydrate, 0.036 g/L calcium chloride dehydrate, 0.006 g/L citric acid, 0.006 g/L ferric citrate, 0.001 g/L nitrilotriacetic acid, 0.020 g/L sodium carbonate, 2.5 g/L HEPES buffer, 1000x modified Wolfe's mineral, and adjusted using 1 mM KOH base to a final pH of 6.90-6.95 at 25°C. Cyanobacteria colonies were incubated under natural daylight at 25°C for 1-2 weeks for full visible growth. *P. ferrooxidans* cell counts were

quantified using nutrient agar growth plates containing (w/v) 1.5% agarose gel, 0.5% peptone, 0.3% yeast extract, 0.5% sodium chloride in one litre ultrapure deionized water. *P. ferrooxidans* colonies were incubated at 25°C for 3-5 days for full visible growth. Serial dilution was necessary ~10^{-7} – 10^{-9}, using the respective media in which they were grown, and plated at consistent temperature of 25°C, to quantify an accurate number of fully formed and distinct colonies. Optical density using spectrophotometric analysis at 600 nm using 1 mL in 2.5 mL plastic cuvettes was accurate in tracking early exponential to middle plateau growth, but it was not useful in determining cell drop off counts during the death phase or the viable cell counts. Both *M. aeruginosa* and *P. ferrooxidans* cell growth was interpreted by optical density using the 600 nm wavelength range. *M. aeruginosa* was maintained in modified BG-11 and 30°C in water bath with standard fluorescent 48" strip lighting of sufficient blue red wavelength emittance and natural sunlight (Apr. – Sept.). Given the proclivity of *M. aeruginosa* to basify even so under high buffering concentrations (>20 mM HEPES) and after several weeks, 50 uL 6 mM HCl additions were provided to neutralize the growth media. *P. ferrooxidans* was maintained in 10 mM acetate growth media detailed in section 2.3 and purified using nutrient agar plates. Growth media under anaerobic conditions was prepared using anaerobic autoclaved ultrapure water and inoculated through sterile loop isolation. Experimental inoculation of all organisms was performed by pellet isolation of mid to late log phase of 100 mL growth media (at ramp 6 decline 6, 4000 rpm centrifuge using 50 mL sterile falcon tubes) and for singly *P. ferrooxidans*, resuspended under anaerobic conditions using an anaerobic tent. The supernatants were discarded, and pellet washed a total of five times using experimental media, and the remaining concentrated suspension was thoroughly vortexed, quantified using optical density and then used for inoculation of experimental replicates.

2.5 Quantification of Iron, Nitrogen and Phosphate

2.5.1 Ferrous/Ferric Iron Determination

Both Fe (II) and total Fe, were quantified using the Ferrozine spectrophotometric method at 562 nm using 2.5 mL plastic cuvettes timed for peak absorbance at 15 minutes, with a reagent recipe of 1.0 g/L Ferrozine per 12 g/L HEPES (stable for several months and stored in 4°C dark refrigeration) (Stookey 1970). Reduction of soluble ferric iron was performed using 0.126 M hydroxylamine hydrochloride $HONH_3^+Cl^-$ for 30 minutes with periodic vortex, and was doubled to prevent significant interference when under the presence of low (<50 mg/L) experimental nitrite. Digestion of magnetite was carried out by 1.5 M HCl dissolution with constant tube rotation, for over seven days to ensure complete digestion. FeS digestion was carried out by 0.5 M HCl digestion with constant tube rotation for over 72 hours. Soluble ferrous to insoluble ferric oxide quantification was performed by 0.5 M HCl digestion for 24 hours.

2.5.2 Nitrite/Nitrate Determination

Nitrogen nitrate speciation was quantified using both the cadmium HACH Nitraver 5 spectrophotometric method at 504 nm using 10 mL standard square glass cuvettes timed for peak absorbance at 5 minutes, and nitrite by the Griess spectrophotometric method at 540 nm using 2.5 mL plastic cuvettes timed for peak absorbance at 20 minutes. 100 uL of sample containing nitrite were diluted into 900 uL H_2O, with 50 uL of Griess (1 mL NEDD stock and 1 mL sulfanilamide stock). Nitrate determination by Griess must be primarily reduced to terminal total nitrite using vanadium (III) chloride as reducing agent, and subsequently incubated at 45°C for

no more than 60 minutes to prevent over reduction to nitric oxide. Nitrite was also determined using cadmium HACH Nitriver 3 spectrophotometric method at 507 nm using 2.5 mL plastic cuvettes timed for peak absorbance at 5 minutes. The Griess method was utilized to prevent complexation/interference with ferrous iron in solution during the HACH method.

2.5.2.1 Preparation of VCl_3 Reducing Agent, NEDD stock and Sulfanilamide stock (Griess)

(1) Fresh 99% purity VCl_3 oversaturated reduction solution was prepared by dissolving 800 mg into 20 mL of ultra-pure distilled water with 8.4 mL HCl (37 wt.%) and topped off to 100 mL, leading to a particle free solution as outlined by Schnetger and Lehners, 2014. The VCl_3 stock was mixed using stir bar for 2 hours until complete dissolution, and then filter sterilized in order to remove any present impurities. (2) The NEDD solution was prepared by using 100 mg N-1-naphthylethylenediamine dihydrochloride (NEDD) was dissolved and dissolved into 100 mL ultrapure water. (3) The sulfanilamide (2%) solution was prepared by dissolving 2.0 g sulfanilamide into a 10% (v/v) HCl solution of 100 mL distilled water solution. (4) Sulfamic acid for pre-treatment was produced by dissolving 583 mg of sulfamic acid into 100 mL ultrapure water solution. The VCl_3 reduction solution was stored and is stable for one month in 4°C dark refrigeration. The remaining three solutions are stable and were stored in 4°C dark refrigeration for a few weeks.

2.5.2.2 Preparation of Vanadium Chloride Reagent Mix and Test

Nitrate determination by conversion to nitrite, in the presence of pre-existing nitrite was performed using the vanadium chloride reagent solution mix (Schnetger and Lehners, 2014), which was prepared using 5 mL of a stock solution of vanadium (III) chloride (purchased fresh as oxidation appears after a few years), 1 mL of stock NEDD, 1 mL sulfanilamide stock (Griess). All three solutions must be at room temperature before application. A sample pre-treatment is required (Cecchini and Caputo, 2010) to remove the pre-existing nitrite from solution inside a 2.5 mL microtube, whereby 30 uL of 60 mM sulfamic acid was added to 500 uL H_2O and 100 uL of sample, then vortexed for 1 minute, and incubated for 15 minutes in the dark at room temperature 25°C (this demonstrated complete removal of nitrite at up to 100 ppm). After pre-treatment, 370 uL of reagent solution mix was added, vortexed for 1 minute, and then incubated at 45°C for no longer than 60 minutes (or 10-20h at room temperature 25°C). After the 60 minute incubation period total reduction is achieved, and the samples were cooled for 5 minutes until they achieved room temperature 25°C. After which, the samples were added to 2.5 mL cuvettes and then read using a spectrophotometer at 540 nm as nitrite. Total nitrate is determined by the reduction ratio NO_3:NO_2, 1:1.

2.5.3 Phosphate Determination

Phosphate determination was carried out by a modified molybdate blue reagent mix and method by spectrophotometric analysis, stable down to 0.1 mg/L PO_4, with ascorbic acid as reducing agent. To prevent significant interference with ferric iron, the L-ascorbic acid reducing agent concentration was doubled. Spectrophotometric analyses were carried out at 882 nm, using 0.1 mL of sample, 0.7 mL of H_2O and 0.2 mL of reagent mix, shaken vigorously, incubated for 5

minutes (absorbance peak was consistently 5 minutes, after heavy shaking for approximately thirty seconds) at room temperature 25°C and read in 2.5 mL plastic cuvette. Microfiltration (0.2 um) of the sample was carried out to determine soluble phosphate and not performed when determining total phosphate (to include phosphate held on ferric iron produced during experiment).

2.5.3.1 Preparation of the Modified Molybdate Blue Reagent Mix

The reagent mix was prepared by mixing (1) 0.0264 g (2x) L-ascorbic acid, (2) 1.25 mL 6.0 M H_2SO_4, (3) 0.375 mL ammonium molybdate, (4) 0.750 mL of ultrapure distilled water and 0.175 mL KSB tartrate. The ammonium molybdate solution was prepared by adding 20.0 g of ammonium molybdate into 500 mL H_2O, and the KSB tartrate solution was prepared by mixing 0.2734 g in 100 mL of H_2O. The solutions were stored in Pyrex bottes, and dark refrigerated at 4°C (Towns 1986).

2.6 Geochemical Modelling

The activity of dissolved species and the degree of saturation for specific minerals (termed saturation index, SI) in the culture medium were determined using the geochemical computer program PHREEQC version 2.18.5570. SI is defined by SI = log (IAP/Ksp), where IAP is the ion activity product of the dissolved mineral constituents and Ksp is the solubility product of the mineral. That is to say, SI > 0 implies oversaturation with measure dependent

natural tendency to precipitate given the absence of kinetic barriers, with respect to the mineral, whereas SI < 0 implies undersaturation.

2.7 Mineralogy and Morphology of Secondary Precipitates

The minerology and morphology of the secondary precipitates qualification were determined with a Rigaku X-ray diffraction (low scan speed, 2θ (0-80°)) and a JOEL scanning electron microscope, respectively. All mineral analysis were done under atmospheric conditions, given that the iron redox experimental systems largely contained oxygen and other redox-reactive species over long periods of time.

3. Results

3.1 *M. aeruginosa* metabolism

M. aeruginosa in modified BG-11 were shown to grow and denitrify at very slow rates (~150 mg/L NO_3) over a single month period. The non-toxin producing strain, reached exponential growth and rapid cell division by a two week period (Figure 3.1). The toxin producing strain reached exponential growth and rapid cell division by over a three week period (Figure 3.2).

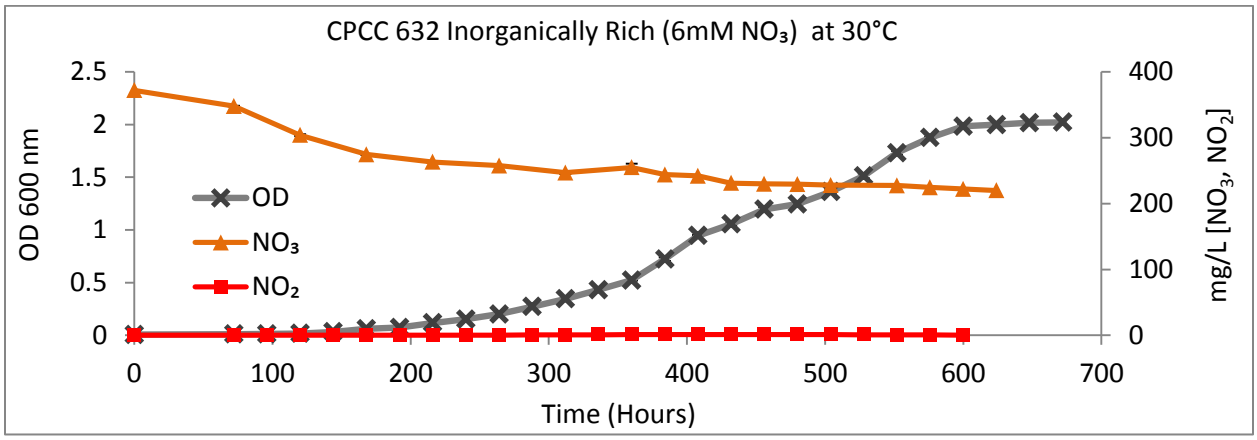

Figure 3.1 – *M. aeruginosa* CPCC 632 (Non-toxin producing) growth curve as optical density in modified BG-11 media, over a thirty day period with a general trend of slow rate denitrification. Error bars represent σ (standard deviation) of mean of triplicate. Error bars too small to be displayed are hidden behind symbol.

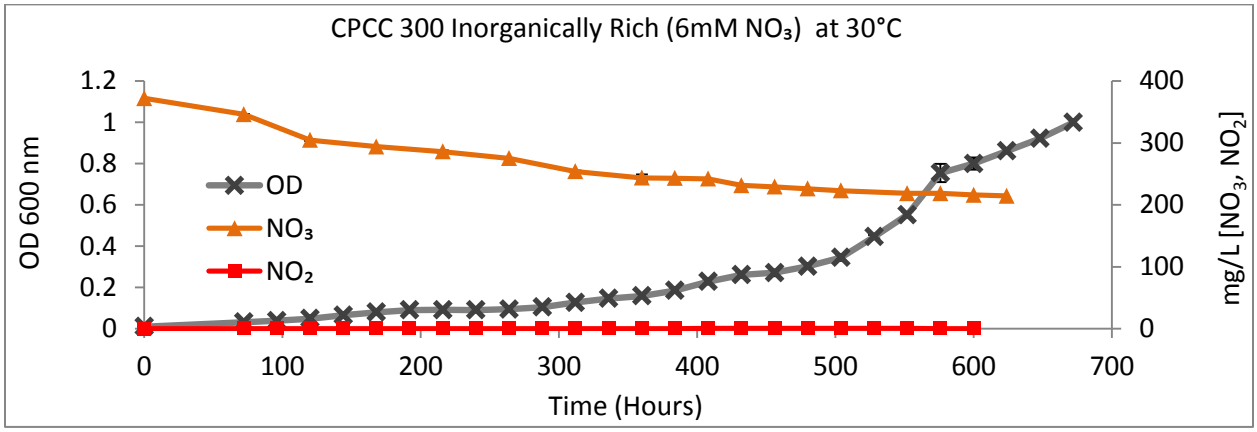

Figure 3.2 – *M. aeruginosa* CPCC 300 (toxin producing) growth curve as optical density in modified BG-11 media, over a thirty day period with a general trend of slow rate denitrification. Error bars represent σ (standard deviation) of mean of triplicate. Error bars too small to be displayed are hidden behind symbol.

3.2 *P. ferrooxidans* metabolism

Nitrate Reducing Iron Oxidizer (NRIO), *P. ferrooxidans* under dissolved oxygen conditions showed little denitrification (178 mg/L NO_3) and slow growth. *P. ferrooxidans* in 18.5 mg/L DO took approximately 48 hours to reach exponential growth and rapid cell division

(Figure 3.3). In anoxia however, the bacteria showed rapid denitrification (as much as 10 mM NO_3) under twenty four hours. The bacteria in </= 0.5 mg/L DO, took approximately 10 hours to reach exponential growth and rapid cell division (Figure 3.4).

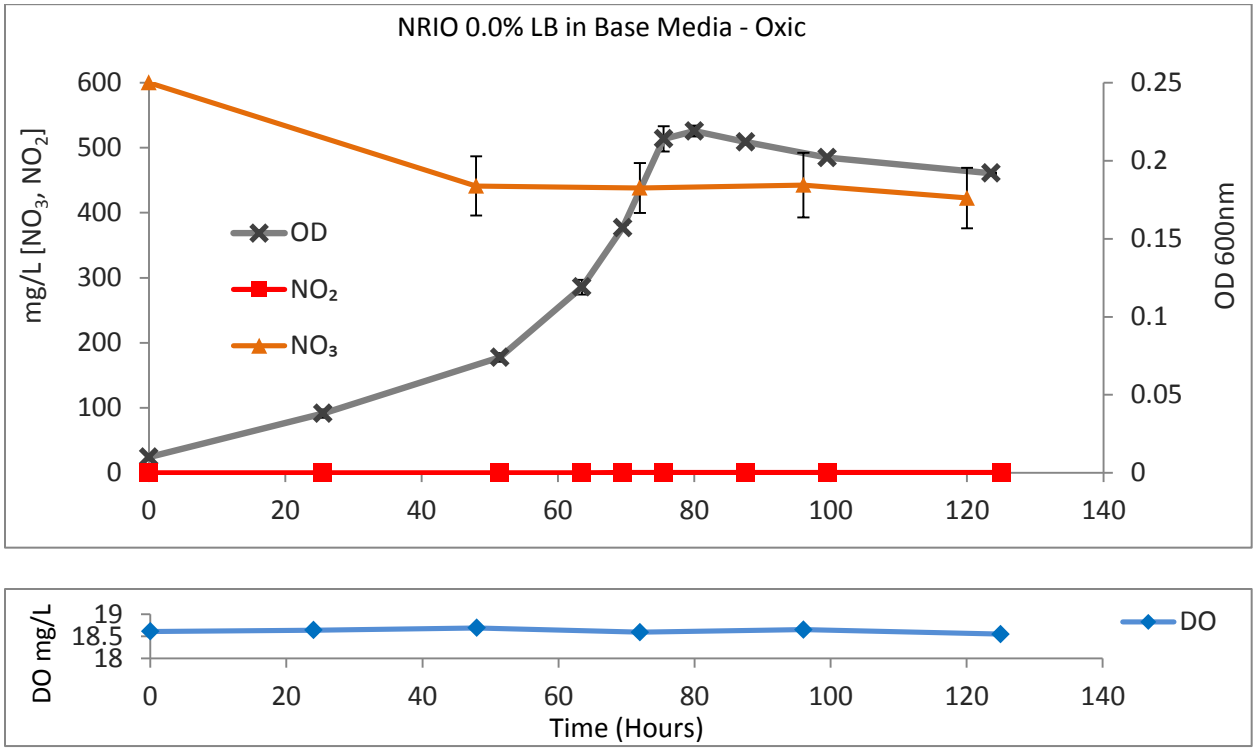

Figure 3.3 – *P. ferrooxidans* growth curve as optical density in modified denitrifying media of phosphorus and nitrogen enrichment with a general absence of denitrification under aerobic atmosphere (>18.0 mg/L DO) at 30°C, over a five day period. Error bars represent σ (standard deviation) of mean of triplicate. Error bars too small to be displayed are hidden behind symbol.

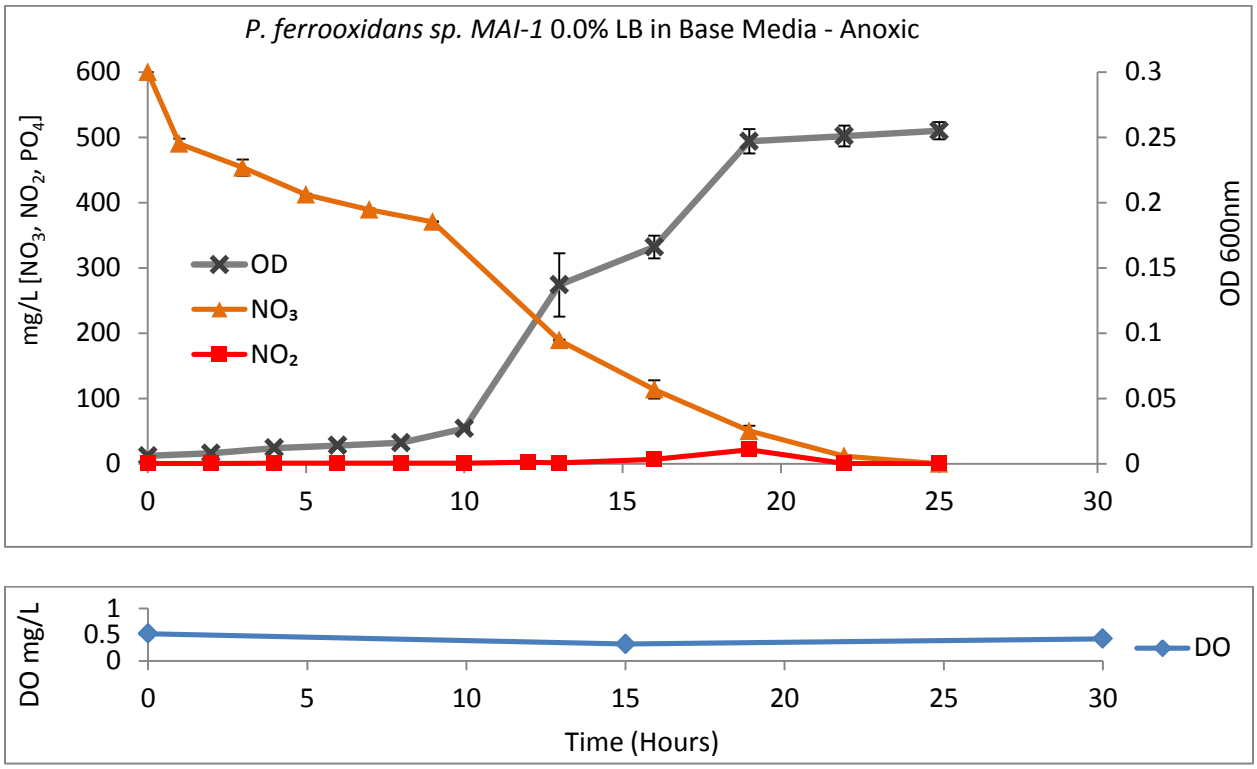

Figure 3.4 - *P. ferrooxidans* growth curve as optical density in modified denitrifying media of phosphorus and nitrogen enrichment with rapid denitrification under anaerobic atmosphere (<1.0 mg/L DO) at 30°C, under a 24 hour period. Pellet OD 600nm: 1.567. Error bars represent σ (standard deviation) of mean of triplicate. Error bars too small to be displayed are hidden behind symbol.

3.3 Interspecific Diffusion Competition (non-toxin)

3.3.1 Cell Counts (CFU/mL) Competitiveness

P. ferrooxidans in competition with non-toxin *M. aeruginosa*, was highly successful in abating a toxic bloom with a powerfully significant decrease in cell counts of *M. aeruginosa* (1.20E+8) by day 15 compared to the control (Figure 3.5). This continued onto day 18 with a cell counts difference of (1.4E+8) compared to the control. *P. ferrooxidans* showed rapid exponential growth and rapid cell death, compared to that of the slow exponential growth and slow cell death of *M. aeruginosa*.

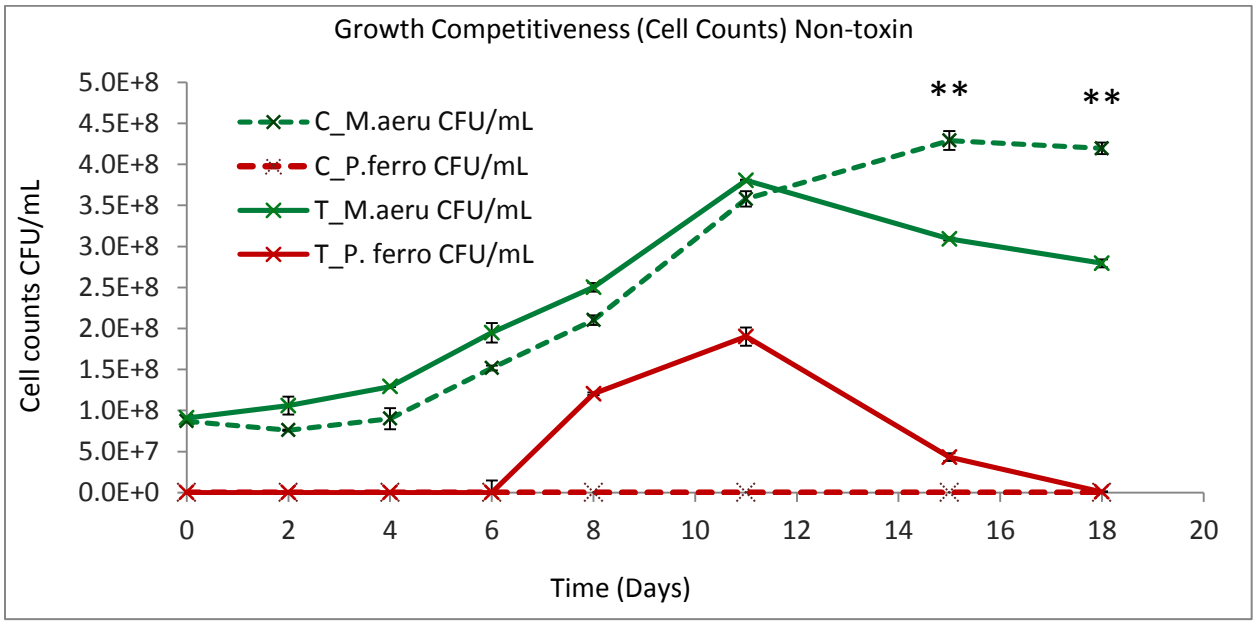

Figure 3.5 - *P. ferrooxidans* growth curve plotted against *M. aeruginosa* growth curve under competition chamber as colony forming units in modified denitrifying media of phosphorus (>0.1 mg/L PO_4) and nitrogen enrichment (<5 mM NO_3) with rapid growth under micro-aerobic atmosphere (>1.0, <2.0 mg/L DO) at 30°C, under a 18 day period. In dotted green CFU/mL *M. aeruginosa* control, in solid green CFU/mL *M. aeruginosa* treatment, in dotted red CFU/mL *P. ferrooxidans* control, in solid red CFU/mL *P. ferrooxidans* treatment. Star above data point indicates significance (p>0.05). Two stars above data point indicates high significance (p>0.01). Error bars represent σ (standard deviation) of mean of triplicate. Error bars too small to be displayed are hidden behind symbol.

3.3.2 Nitrate Competitiveness (non-toxin)

P. ferrooxidans against non-toxin *M. aeruginosa* showed rapid denitrification under micro-aerobic atmosphere by day 7 (>1.0, <2.0 mg/L DO) at 30°C, and continued over a 16 day total period. A total of > 3.5 mM NO_3 was removed from the system after 16 days, owed to microbial competition (Figure 3.6).

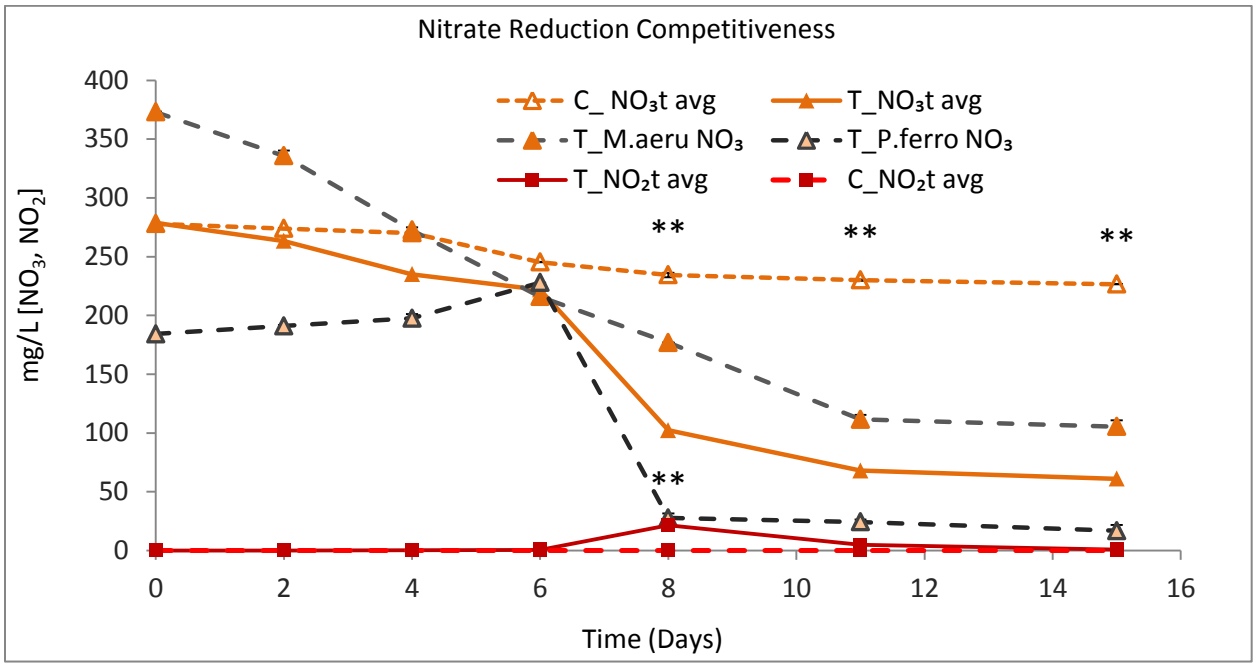

Figure 3.6 - *P. ferrooxidans* nitrogen denitrification plotted against *M. aeruginosa* nitrogen denitrification under competition chamber as nitrate, nitrite in modified denitrifying media of phosphorus (>0.1 mg/L PO_4) and nitrogen enrichment (<5 mM NO_3). In dotted orange control total nitrate average, in solid orange treatment total nitrate average, in solid red treatment total nitrite of system, in dotted red treatment total nitrite of system, in dotted gray solid orange triangle treatment nitrate of *M. aeruginosa*, in dotted black bordered black triangle treatment nitrate *P. ferrooxidans*. Star above data point indicates high significance (p>0.05). Two stars above data point indicates high significance (p>0.01). Error bars represent σ (standard deviation) of mean of triplicate. Error bars too small to be displayed are hidden behind symbol.

3.3.3 Phosphate Competitiveness (non-toxin)

P. ferrooxidans against non-toxin *M. aeruginosa* showed rapid abiotic precipitation of phosphate-rich minerals and slow biotic assimilation under micro-aerobic atmosphere (>1.0, <2.0 mg/L DO) at 30°C, under a 18 day total period. The difference in microbial competition for total phosphate in the system was ~0.1 mg/L PO_4 (Figure 3.7).

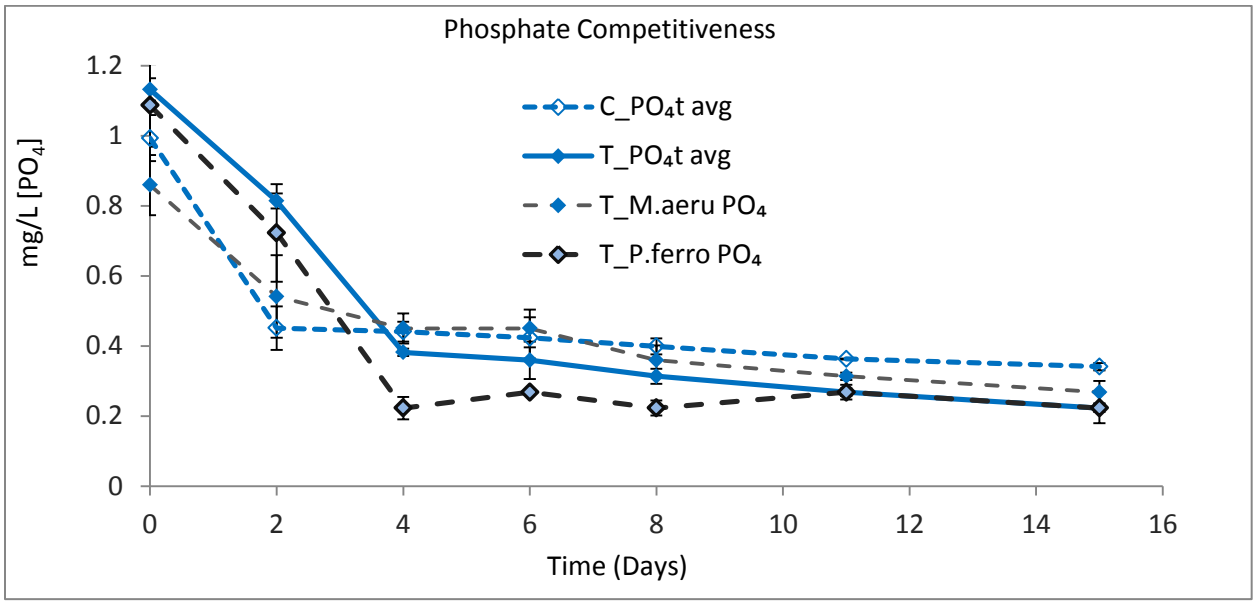

Figure 3.7 - *P. ferrooxidans* phosphorus assimilation plotted against *M. aeruginosa* phosphorus assimilation under competition chamber as inorganic phosphate in modified denitrifying media of phosphorus (>0.1 mg/L PO_4) and nitrogen enrichment (<5 mM NO_3). In dotted blue control total phosphate average of system, in solid blue treatment total phosphate average of system, in dotted gray treatment phosphate *M. aeruginosa*, in dotted black black border diamond treatment phosphate of *P. ferrooxidans*. Error bars represent σ (standard deviation) of mean of triplicate. Error bars too small to be displayed are hidden behind symbol.

3.3.4 Geochemical Model and Saturation Indices

The geochemical model obtained from PHREEQC showed that vivianite and several Fe (III) oxides, namely, hematite, goethite, iron hydroxide and k-jarosite, have the potential to precipitate (Table 3.1).

Table 3.1 – Geochemical model qualitative phase generation of treatment non-toxin producing competition experiment at time = 0, with associated saturation indices (SI), log IAPs and log KTs. A positive value, SI > 0, IAP > K_{sp}, indicates a measure dependent proclivity to oversaturate (supersaturated). A negative value, SI < 0, IAP < K_{sp}, indicates a measure dependent proclivity to remain unformed (undersaturated). IAP = K_{sp}, SI = 0, is saturated (in equilibrium). Saturation index is calculated by the log of IAP (ion activation product) divided by KT or K_{sp} (equilibrium constant).

t_0	Phase	SI	log IAP	log KT	
	Anhydrite	-2.24	-6.62	-4.39	$CaSO_4$
	Gypsum	-2.04	-6.62	-4.58	$CaSO_4:2H_2O$
	$H_2(g)$	-22.00	-25.17	-3.17	H_2
	$H_2O(g)$	-1.38	-0.00	1.38	H_2O
	Halite	-5.51	-3.92	1.59	NaCl
	Hydroxyapatite	-3.06	-6.92	-3.86	$Ca_5(PO_4)_3OH$
	Melanterite	-4.30	-6.45	-2.15	$FeSO_4:7H_2O$
	$NH_3(g)$	-7.25	-5.58	1.67	NH_3
	$O_2(g)$	-1.50	-4.42	-2.93	O_2
	Vivianite	**3.80**	**-32.20**	**-36.00**	**$Fe_3(PO_4)_2:8H_2O$**
	Fe(OH)3(a)	**3.43**	**8.33**	**4.89**	**$Fe(OH)_3$**
	Goethite	**9.33**	**8.33**	**-1.00**	**FeOOH**
	Hematite	**20.66**	**16.65**	**-4.01**	**Fe_2O_3**
	Jarosite-K	**2.53**	**-6.68**	**-9.21**	**$KFe_3(SO_4)_2(OH)_6$**

3.3.5 X-Ray diffraction Pattern (non-toxin)

The X-Ray diffraction pattern obtained from a non-pooled secondary mineral produced from the treatment non-toxin competition experiment showed Fe (III) – hydroxide (11.9, 27.0, 38.0, 52.9, 61.0 deg.), vivianite (6.9, 11.9 deg.), hematite goethite (38.0, 39.1, 68.1, 70.0 deg.), with the possibility of k-jarosite masked in the mineral pattern background (Figure 3.8).

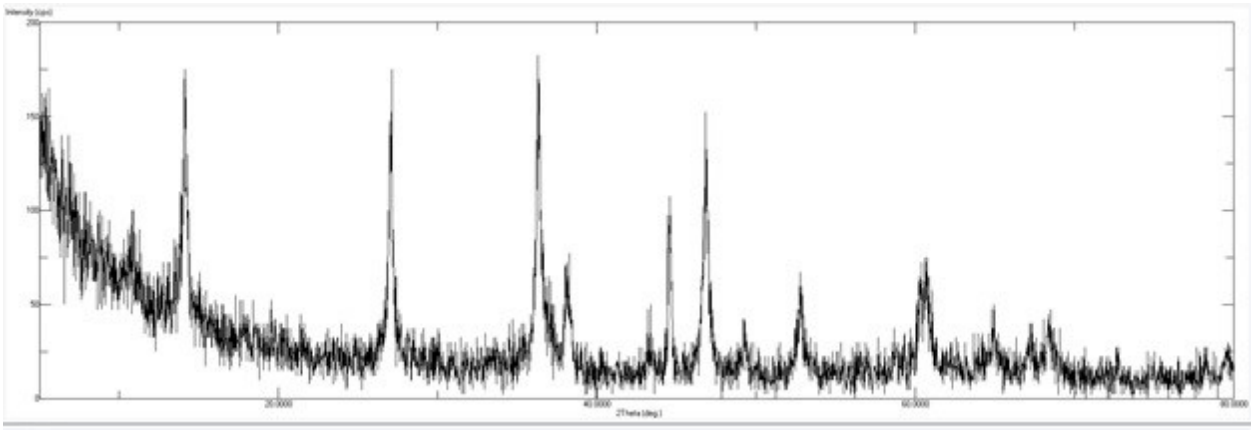

Figure 3.8 – A non-destructive slow scan X-Ray diffraction profile in x-axis 2θ (0-80°), versus y-axis intensity counts per second (cps) 0-200.

3.3.6 Ferrous Iron versus Total Reduced Ferrous Iron (non-toxin)

Abiotic and biotic oxidation (post day 7) of Fe (II) was shown to occur over a two week period under micro-aerobic atmosphere (>1.0, <2.0 mg/L DO) at 30°C (Figure 3.9). Calculated saturation indices for vivianite at day 0 (i.e., SI = 3.80) and day 8 (i.e., S.I. = 0.44) were positive, indicating that vivianite lilely contributed to the removal of Fe in solution through precipitation.

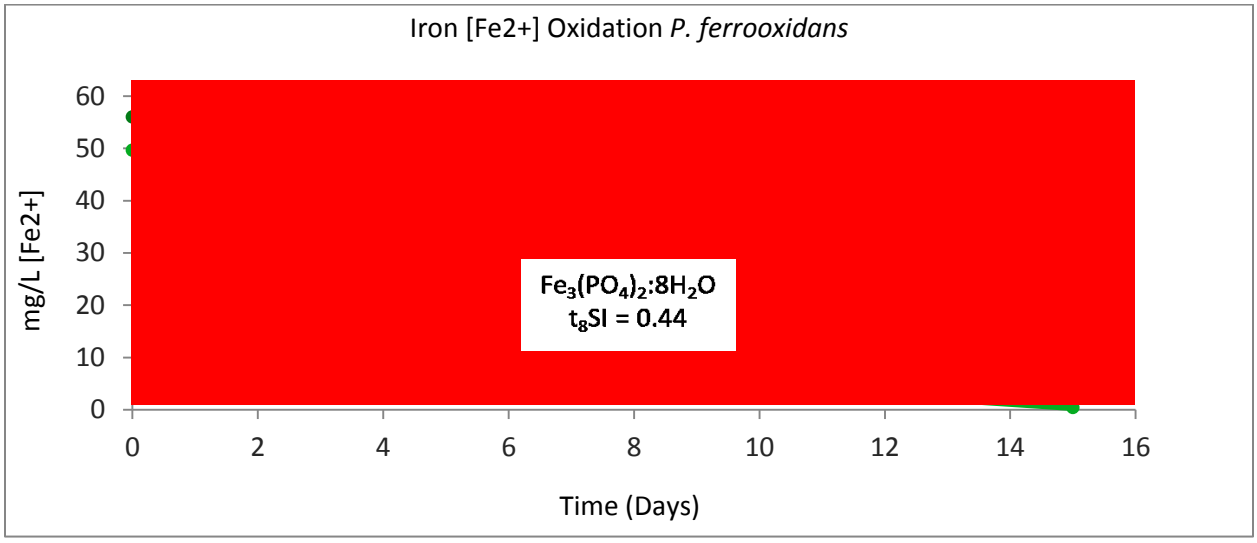

Figure 3.9 – Iron oxidation of competition experiment by *P. ferrooxidans* and abiotic oxygen. In dotted green line total ferrous/ferric iron reduced by hydroxylamine hydrochloride, in solid green line total ferrous iron. S.I. values for vivianite are indicated for days 0 and 8. Error bars represent σ (standard deviation) of mean of triplicate. Error bars too small to be displayed are hidden behind symbol.

3.4 Interspecific Diffusion Competition (toxin)

3.4.1 Cell Counts (CFU/mL) Competitiveness

P. ferrooxidans in competition with the non-toxin *M. aeruginosa*, was highly successful in abating a toxic bloom with a powerfully significant decrease in cell counts of *M. aeruginosa* (6.93E+7) by day 15 compared to the control (Figure 3.10). This continued onto day 18 with a cell counts difference of (1.12E+8) compared to the control. *P. ferrooxidans* showed rapid exponential growth and rapid cell death, compared to that of the slow exponential growth and slow cell death of *M. aeruginosa*.

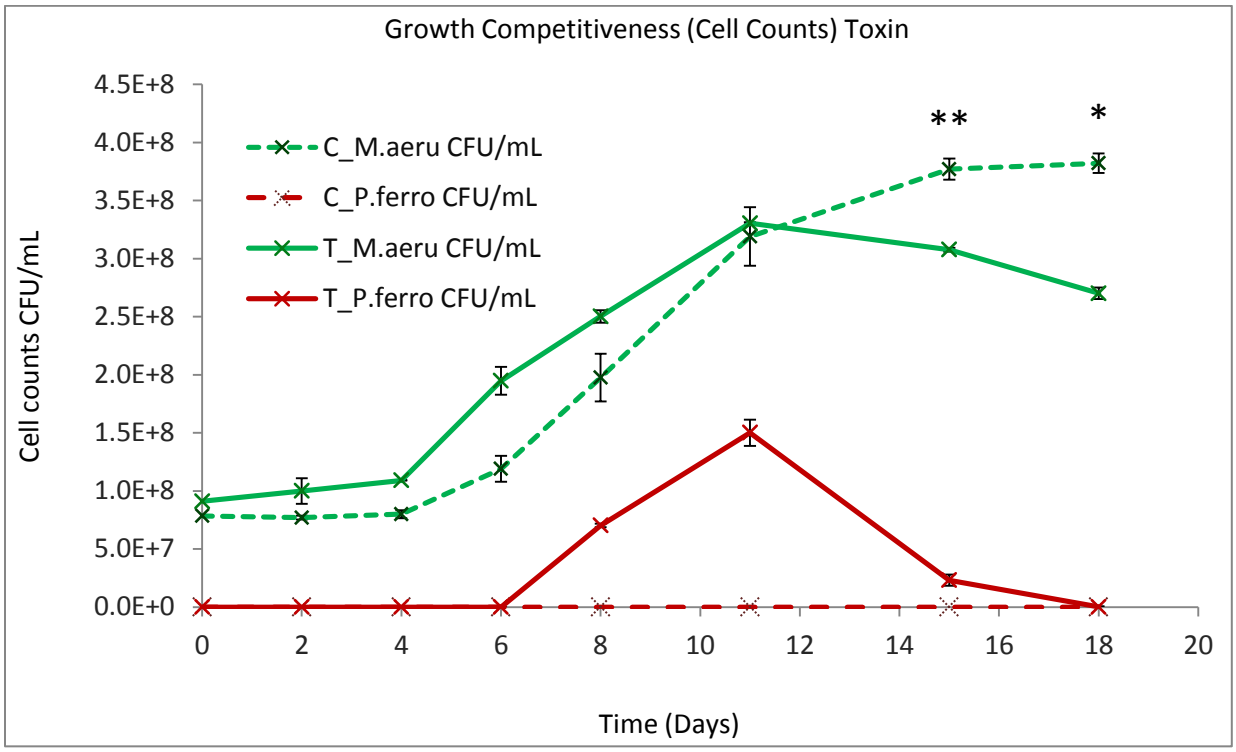

Figure 3.10 - *P. ferrooxidans* growth curve plotted against *M. aeruginosa* growth curve under competition chamber as colony forming units in modified denitrifying media of phosphorus (>0.1 mg/L PO_4) and nitrogen enrichment (<5 mM NO_3) with rapid growth under micro-aerobic atmosphere (>1.0, <2.0 mg/L DO) at 30°C, under a 18 day period. In dotted green CFU/mL *M. aeruginosa* toxic control, in solid green CFU/mL *M. aeruginosa* toxic treatment, in dotted red CFU/mL *P. ferrooxidans* control, in solid red CFU/mL *P. ferrooxidans* treatment. Star above data point indicates significance (p>0.05). Two stars above data point indicates high significance (p>0.01). Error bars represent σ (standard deviation) of mean of triplicate. Error bars too small to be displayed are hidden behind symbol.

3.4.2 Nitrate Competitiveness (toxin)

P. ferrooxidans against the toxin producing *M. aeruginosa* showed rapid denitrification under micro-aerobic atmosphere by day 7 (>1.0, <2.0 mg/L DO) at 30°C, and continued over a 16 day total period. A total of > 3.5 mM NO_3 was removed from the system after 16 days, owing to microbial competition (Figure 3.11).

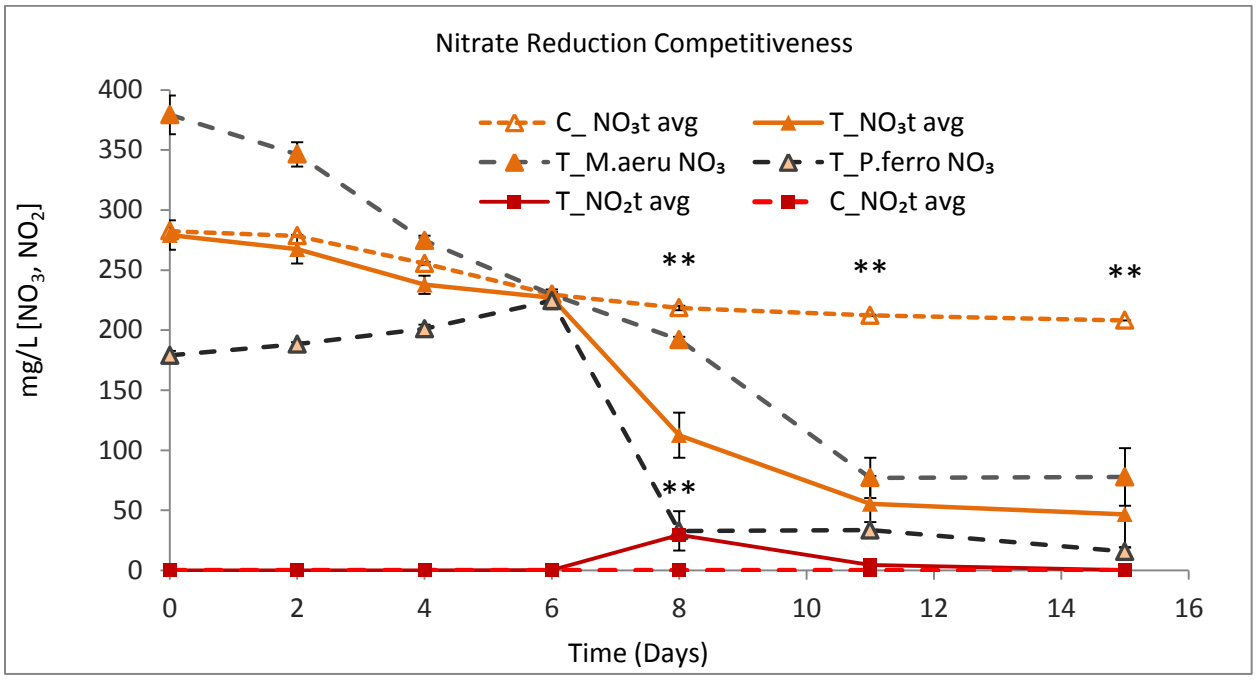

Figure 3.11 - *P. ferrooxidans* nitrogen denitrification plotted against toxic *M. aeruginosa* nitrogen denitrification under competition chamber as nitrate, nitrite in modified denitrifying media of phosphorus (>0.1 mg/L PO_4) and nitrogen enrichment (<5 mM NO_3). In dotted orange control total nitrate average of system, in solid orange treatment total nitrate average of system, in solid red treatment total nitrite average of system, in dotted red control total nitrite average of system, in dotted gray solid orange triangle treatment nitrate of *M. aeruginosa*, in dotted black bordered black triangle treatment nitrate *P. ferrooxidans*. Star above data point indicates significance (p>0.05). Two stars above data point indicates high significance (p>0.01). Error bars represent σ (standard deviation) of mean of triplicate. Error bars too small to be displayed are hidden behind symbol.

3.4.3 Phosphate Competitiveness (toxin)

P. ferrooxidans against the non-toxin *M. aeruginosa* showed rapid abiotic precipitation and slow biotic assimilation under micro-aerobic atmosphere (>1.0, <2.0 mg/L DO) at 30°C, under a 18 day total period (Figure 3.12). The difference in microbial competition for total phosphate in the system was ~0.1 mg/L PO_4.

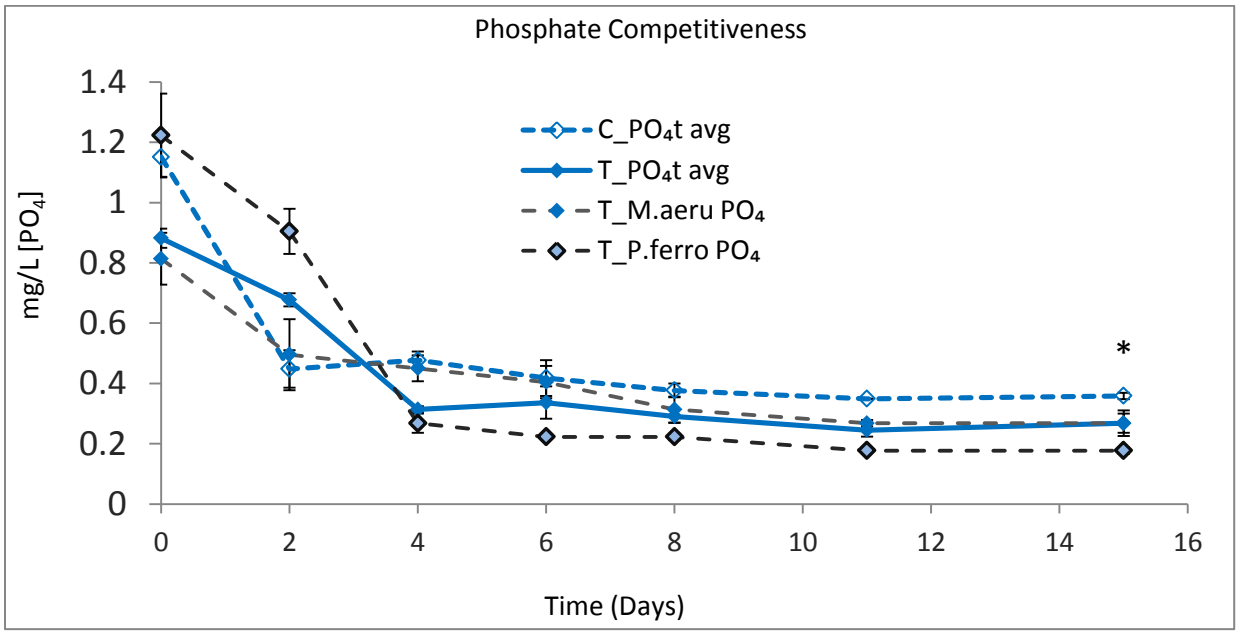

Figure 3.12 - *P. ferrooxidans* phosphorus assimilation plotted against toxic *M. aeruginosa* phosphorus assimilation under competition chamber as inorganic phosphate in modified denitrifying media of phosphorus (>0.1 mg/L PO_4) and nitrogen enrichment (<5 mM NO_3). In dotted blue control total phosphate average of system, in solid blue treatment total phosphate average of system, in dotted gray treatment phosphate *M. aeruginosa*, in dotted black black border diamond treatment phosphate of *P. ferrooxidans*. Star above data point indicates significance (p>0.05). Error bars represent σ (standard deviation) of mean of triplicate. Error bars too small to be displayed are hidden behind symbol.

3.4.4 Geochemical Model and Saturation Indices (toxin)

The geochemical model obtained from PHREEQC showed that vivianite and several Fe (III) oxides, namely, hematite, goethite, iron hydroxide and k-jarosite, had positive S.I. values and therefore the potential to precipitate (Table 3.2).

Table 3.2 – Geochemical model qualitative phase generation of treatment toxin producing competition experiment at time = 0, with associated saturation indices (SI), log IAPs and log KTs. A positive value, SI > 0, IAP > K_{sp}, indicates a measure dependent proclivity to oversaturate (supersaturated). A negative value, SI < 0, IAP < K_{sp}, indicates a measure dependent proclivity to remain unformed (undersaturated). IAP = K_{sp}, SI = 0, is saturated (in equilibrium). Saturation index is calculated by the log of IAP (ion activation product) divided by KT or K_{sp} (equilibrium constant).

t_0	Phase	SI	log IAP	log KT	
	Anhydrite	-2.24	-6.62	-4.39	$CaSO_4$
	Gypsum	-2.04	-6.62	-4.58	$CaSO_4:2H_2O$
	$H_2(g)$	-22.00	-25.17	-3.17	H_2
	$H_2O(g)$	-1.38	-0.00	1.38	H_2O
	Halite	-5.51	-3.92	1.59	NaCl
	Hydroxyapatite	-3.06	-6.92	-3.86	$Ca_5(PO_4)_3OH$
	Melanterite	-4.30	-6.45	-2.15	$FeSO_4:7H_2O$
	$NH_3(g)$	-7.25	-5.58	1.67	NH_3
	$O_2(g)$	-1.50	-4.42	-2.93	O_2
	Vivianite	**3.80**	**-32.20**	**-36.00**	**$Fe_3(PO_4)_2:8H_2O$**
	Fe(OH)3(a)	**3.43**	**8.33**	**4.89**	**$Fe(OH)_3$**
	Goethite	**9.33**	**8.33**	**-1.00**	**FeOOH**
	Hematite	**20.66**	**16.65**	**-4.01**	**Fe_2O_3**
	Jarosite-K	**2.53**	**-6.68**	**-9.21**	**$KFe_3(SO_4)_2(OH)_6$**

3.4.5 X-Ray diffraction Pattern (toxin)

The X-Ray diffraction pattern obtained from a non-pooled secondary mineral produced from the treatment toxin competition experiment showed peaks belonging to vivianite (6.9, 11.9 deg.), Fe (III) – hydroxide (11.9, 27.0, 38.0, 52.9, 61.0 deg.) with lower intense peaks compared

to that of the toxin producing experiment, hematite goethite (38.0, 39.1, 68.1, 70.0 deg.) with the possibility of k-jarosite masked in the mineral pattern background (Figure 3.13).

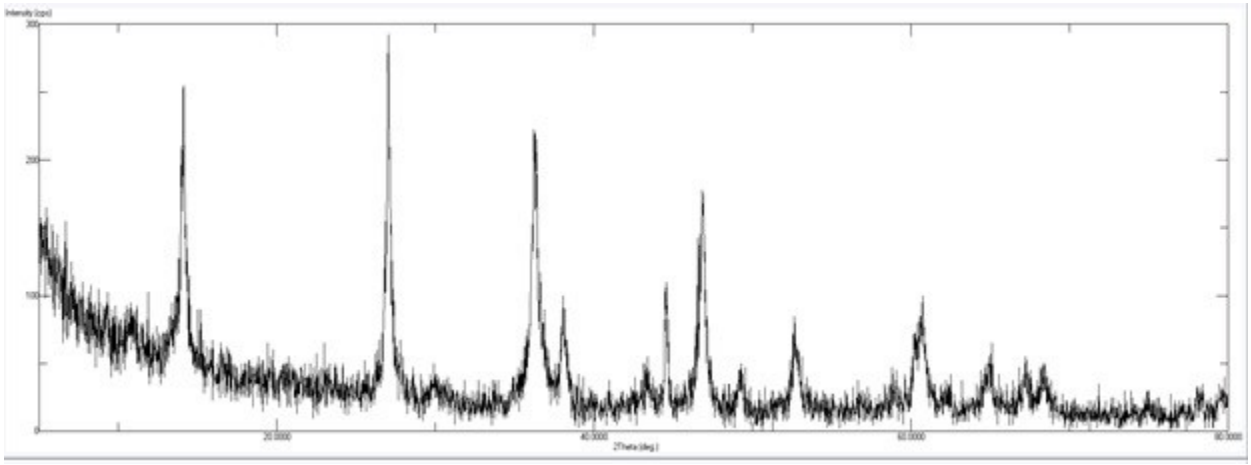

Figure 3.13 – A non-destructive slow scan x-ray diffraction profile in x-axis 2θ (0-80°), versus y-axis intensity counts per second (cps) 0-200.

3.4.6 Ferrous Iron versus Total Reduced Ferrous Iron (toxin)

Abiotic and biotic oxidation (post day 7) of Fe (II) was shown to occur over a two week period under micro-aerobic atmosphere (>1.0, <2.0 mg/L DO) at 30°C. Saturation indices for vivianite at day 0 and day 8 were 3.80 and 0.55, respectively (Figure 3.14). The formation of vivianite likely explained the decline of Fe is solution.

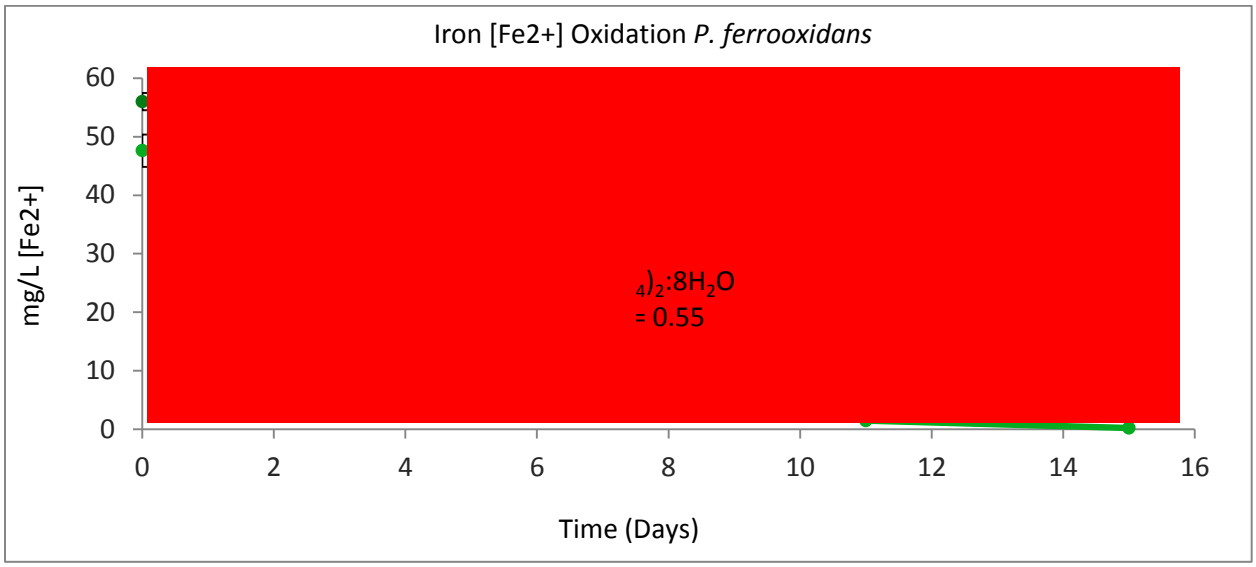

Figure 3.14 – Iron oxidation of competition experiment by *P. ferrooxidans* and abiotic oxygen. In dotted green line total ferrous/ferric iron reduced by hydroxylamine hydrochloride, in solid green line total ferrous iron. Abiotic and biotic *P. ferrooxidans* shows rapid ferrous oxidation, with near complete oxidation over a two week period under micro-aerobic atmosphere (>1.0, <2.0 mg/L DO) at 30°C with positive S.I. values for vivianite. Error bars represent σ (standard deviation) of mean of triplicate. Error bars too small to be displayed are hidden behind symbol

3.4.7 SEM of Secondary Mineral (pooled)

Scanning electron microscope imaging of pooled toxin and non-toxin secondary mineral showed both cuboidal and porous spherical grains, resembling vivianite-metavivianite and various Fe (III) – oxides / hydroxides (Figure 3.15).

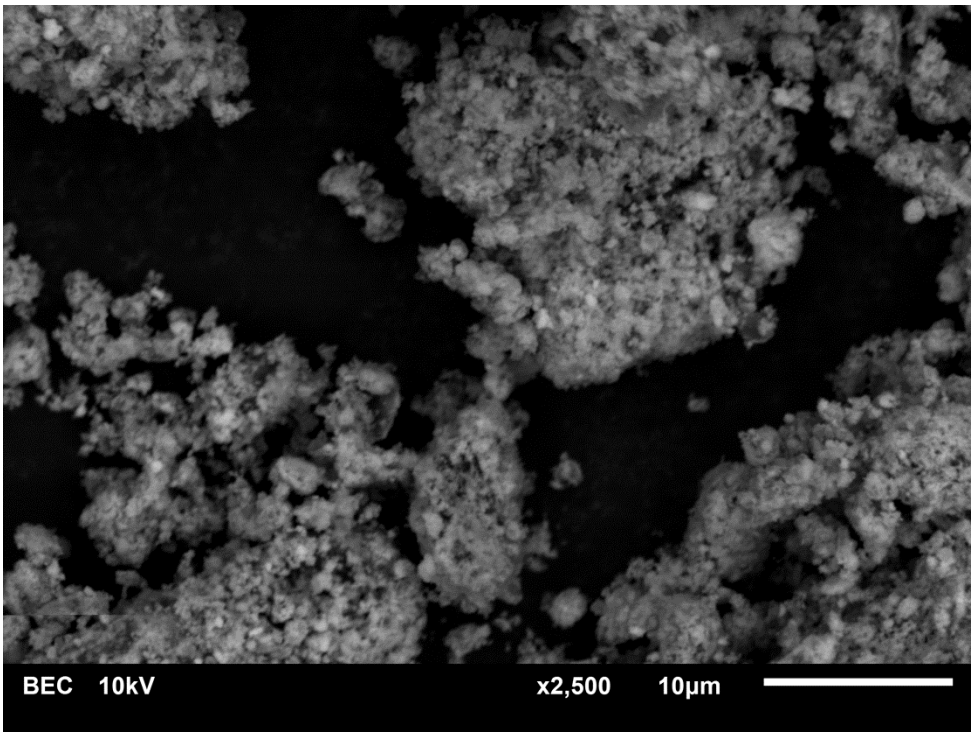

Figure 3.15 - Scanning electron microscopy imaging at low magnification showing fine mineralized to biomineralized iron-rich minerals in the competition chamber containing the modified denitrifying medium.

3.4.8 PXRD2 Model

A geometric pattern was obtained using the PXRD2 software yielding the overall mineral composition. The highest intensities match closely to the iron hydroxide secondary mineral profile followed by vivianite-metavivianite (Figure 3.16). The wideness of the crystallites is indicative of overlapping patterns of several iron oxide minerals that are heterogeneously assorted together.

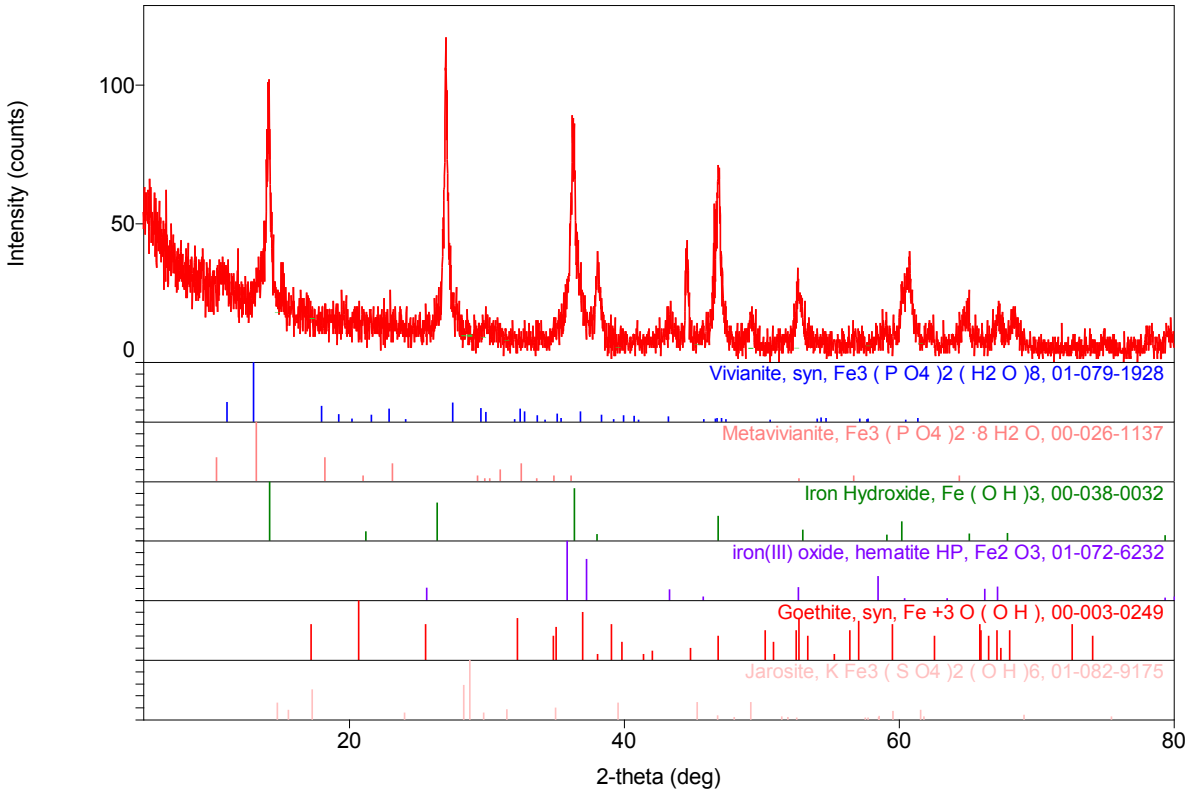

Figure 3.16 –The XRD pattern representing the pooled secondary mineral obtained from both the non toxin and toxin treatment competition experiments (cyanobacteria and *P. ferrooxidans* together) after eighteen days. In blue, vivianite, in pink metavivianite, in green, Fe (III) - hydroxide, in purple, hematite, in red goethite and in orange k-jarosite.

3.5 Single Factor ANOVA Tests

When using *P. ferrooxidans* under iron mono sulfide as electron source, iron was rapidly oxidized with high significance at day 1.08, but this effect diminished and reached a plateau with the loss of nitrate in the system, with no significant effect on the phosphate concentration over a period of 8.25 days (0.120 NS) (Table 3.3). When using *P. ferrooxidans* under a magnetite system, we can see a strong difference in the degree of phosphate assimilation, which is highly

significant by day 4.75 (2.71E-3 **). During the non-toxin and toxin competition experiment, *P. ferrooxidans* and soluble ferrous iron introduced as treatment resulted in a significant rate of denitrification change as opposed to *M. aeruginosa* alone, indicating a significant level of primary metabolite competition by day 15 (5.07E-6 **, 4.12E-7 **), for the non toxin and toxin producing strains, respectively.

Table 3.3 – Measures of time dependent significances based off single factor ANOVAs. One star indicates first significance level at the p>0.05, two stars indicates second significance level at the p>0.01.

Experiment	Iron Source	Character of Comparison	Time (Day)	F	P-value
M. aeruginosa Competition Setting (non-toxin)	1 mM $FeCl_2$	Cell Count CFU/mL of *M. aeruginosa*	15, 18	91.1, 327	6.73E-4, 5.49E-5 **
M. aeruginosa Competition Setting (non-toxin)	1 mM ferrous $FeCl_2$	$[NO_3]$	8, 15	5908.9, 1084.8	1.72E-7, 5.07E-6 **
M. aeruginosa Competition Setting (non-toxin)	1 mM ferrous $FeCl_2$	$[NO_2]$	8	1875.9	1.7E-6 **
M. aeruginosa Competition Setting (non-toxin)	1 mM ferrous $FeCl_2$	$[PO_4]$	15	7.51	0.0518 NS
M. aeruginosa Competition Setting (toxin)	1 mM ferrous $FeCl_2$	Cell Count CFU/mL of *M. aeruginosa*	15, 18	65.1, 16.3	1.28E-3 **, 0.0156 *
M. aeruginosa Competition Setting (toxin)	1 mM ferrous $FeCl_2$	$[NO_3]$	8. 15	230.1, 3811.9	1.1E-7, 4.12E-7 **
M. aeruginosa Competition Setting (toxin)	1 mM ferrous $FeCl_2$	$[NO_2]$	8	91.2	6.7E-4 **
M. aeruginosa Competition Setting (toxin)	1 mM ferrous $FeCl_2$	$[PO_4]$	15	12.67	0.0236 *

3.6 Summary of Kinetic Parameters

When using *P. ferrooxidans* under a euxinic system the assimilation rate of nitrogen-nitrate was nearly the double the rate of the magnetite system (3.50E-5), and nearly eight times that of the microaerophilic interface system (1.28E-5), indicating that nitrogen assimilation through the process of iron mono sulfide may be highly favorable toward the microorganismal metabolic speed (Table 3.4). *M. aeruginosa* nitrate and phosphate assimilation were very slow during the pre-exponential phase, and generally speaking increase by at least a factor of ten during the rapid growth phase, for both non toxin and toxin producing strains.

Table 3.4 – Mean inorganic assimilation rates minus control linear triplicate component with associated microorganisms, carbon and iron source. Rate = ΔC/Δt

Experimental Conditions				Kinetic Parameters			
Competition Setting (non-toxin >1uM P)	*P. ferrooxidans*	1 mM $FeCl_2$	5 mM C as acetate	NO_3	6-15	NA	1.28E-5
Competition Setting (toxin > 1uM P)	*P. ferrooxidans*	1 mM $FeCl_2$	5 mM C as acetate	NO_3	6-15	NA	1.49E-5
Competition Setting (non-toxin >1uM P)	*M. aeruginosa* 632	NA	Atm.	NO_3	0-4, 4-11	2.85E-6	2.08E--6
Competition Setting (toxin >1uM P)	*M. aeruginosa* 300	NA	Atm.	NO_3	0-4, 4-11	7.36E-7	2.01E-6
Denitrifying Media (1uM-10uM P)	*M. aeruginosa* 632	NA	Atm.	PO_4	9-18, 19-26	4.88E-9	1.57E-8
Denitrifying Media	*M. aeruginos*	NA	Atm.	PO_4	9-18, 19-26	1.46E-8	1.88E-8

(1uM-10uM P)	*a* 300	

4. Discussion

4.1 *M. aeruginosa* and *P. ferrooxidans* Interspecific Competition Experiment

4.1.1 M. aeruginosa Niche Dominance

Microcystis aeruginosa are prepotent and highly competitive ancient cyanobacteria, such that their method of dominating a niche incorporates a diverse variety of interspecific effective mechanisms. They are primarily P-phosphate dependent in terms of rate, density and longevity of growth and can be sustained for long periods of time, upward of several years when nutrients are sufficient (Schindler et al. 2008; Schindler et al. 1997). When in abundance they are also proactive and quickly assimilate inorganic nutrients. Little is known about how cyanobacteria perform under denitrifying competition communities under low level enrichments of phosphate (<1.0 mg/L, >0.1 mg/L PO_4). Under nitrate reduction by way of heterospecific competition, nitrogen removal rates successfully abated cyanotoxic blooms and cultivability (Figure 3.5, 3.10), which suggests high N-nitrate dependency under low level enrichments of phosphorus. For instance, when cyanobacteria are present under high levels of bioavailable phosphate, and by way of internalization for low phosphate, this triggers rapid and prolific dominance and decreases the cyanobacteria's nitrogen dependence (Ernst et al. 2005; Hudek et al. 2016; Schindler et al. 2008). Provided sufficient light is present for dependent respiration (Utkilen and Gjolme, 1992), trace mineral metals are biologically accessible (Morissey and Bowler, 2012), and a sustained warm mesophilic environment exist; cyanobacteria diminish aquatic ecosystem and may also diminish microbial diversity by rapid nutrient uptake or by means of phosphatase

inhibition (Levy 2017). Cyanobacteria blooms also generate indirect oxygen depletion, and are capable of proliferated to all levels of the aquatic environment (Levy 2017). Cyanobacteria blooms generate corollary eutrophication and and subsequent benthic maturation (Levy 2017). They are also known to produce concomitant nitrogen dependent microcystin production (Levy 2017). Microcystins produced by *M. aeruginosa* are dangerous heptapeptides, and have been shown to inhibit protein phosphatases common in many microorganisms, induce oxidative stress, damage nucleic acid structures including DNA, mitochondrial function, cause cytoskeleton disruption, organelle disruption and are known to trigger programmed cell death pathways as apoptosis (Chen and Xie, 2016). Organ toxicity has also been examined in zebra mussels introduced as primary predation; vertebrate toxicity such as fish and humans in the form of liver and nervous tissue impair and cell death, as well as aquatic zooplankton consumption shifts (Azevedo et al. 2002; Galloway et al. 2008; Steffen et al. 2014). In order to prevent *M. aeruginosa* spread, one option remains: (1) the reduction of nutrient input to aquatic bodies and reservoirs. Little has been investigated in regards to the discovery of a novel competitor. Long term mitigation strategies of *M. aeruginosa* by removing cyanobacteria through induced aggregation have demonstrated to be largely ineffectual (Steffen et al. 2014), for provided uncontrolled anthropogenic fluxes are sustained within an ecosystem, the function of primary bioremediation by *M. aeruginosa* in the form of toxic cyanobacterial blooms will continue to arise. Future strategies should be focused on removing nutrients and strategies intimately tied to microbial competition mechanisms, rather than the dominantly reoccurring organism itself.

4.1.2 M. aeruginosa Microcystin Production

M. aeruginosa strain CPCC 300, isolated from the Pretzlaff pond in Alberta, has been characterized to produce as much as 204 ug/L microcystin. Compared to the non-toxic experiment, the peak logarythmic growth of *P. ferrooxidans* did not pass the first significance level of difference $p>0.05$ with a p value of 0.194 and F value of 2.43 and critical value of 7.71. However, because microcystins were not quantified, cytotoxicity could not be determined and was not further explored. Microcystins are small hepatotoxins (nanometer range) much smaller than the experimental diffusion filter pore interface (0.2 um), and in terms of size can permeate (Levy 2017). However, given the heptatoxin's polarity (Levy 2017), it is possible that the microcystins may have been entrapped at porous interface. Future research should focus on the plausible chemical adhesiveness of microcystins to filter pores and should work to develop an effective approach to concentrate and quantify microcystins of this study type.

4.1.3 P. ferrooxidans Nutrient and Growth Competitiveness against M. aeruginosa

Growth competition of non-toxin strain *M. aeruginosa* (pellet OD 600nm: *M. aeruginosa* Treatment1.897, Control 1.991; *P. ferrooxidans* T 1.432) demonstrated significant growth inhibition by day 15, and continued onto day 18 dually at the second significance level $p>0.01$, as highly significant (Figure 3.5). The toxin producing strain (pellet OD 600nm: *M. aeruginosa* Treatment 1.798, Control 1.877; *P. ferrooxidans* T 1.347) produced similar results and demonstrated growth inhibition by day 15 (Figure 3.10) at the second significance level >0.01, and was not sustained onto day 18, but continued with the first significance level $p>0.05$ up to 0.0156. This largely could owe to toxin production, but however did not in turn reduce competition of primarily metabolites such as primary phosphate and nitrogen. It is important to

mention that betaproteobacteria and generally, iron oxidizing bacteria, are suspected to have co-existed with ancient cyanobacteria since the inception of the Neoarchean in deep water Archean oceans, such that future research of their current relationship in namely, lake Matano and other Archean facsimiles, may further detail the interplay between competition and community. For both *M aeruginosa* experiments, overall nitrogen competition differed by >500x more than to P-phosphate removal, which largely surpasses the suggested nitrogen removal rates of 4:1 N:P reduction to diminish toxin bloom formations, outlined by Schindler et al. 2008. That is to say, it is standardized to focus on reducing phosphate as a primary remediation aim rather than focusing on reducing nitrogen by a factor of four times more. It therefore becomes much more difficult as nitrogen requires more of an economic and laborious expenditure to abate a bloom. Focusing on nitrogen alone could also lead to selection of N-fixing strains (Schindler et al. 2018). However under rapid removal by NDFe(II)OB for example, total treatment nitrate reduction over duration of non-toxin competition (>3.5 mM, 217.56 mg/L NO_3) was highly significant by day 8 to 15 at $p>0.01$ (Figure 3.6), and showed no phosphate significant difference post *P. ferrooxidans* inoculation. Total treatment nitrate reduction over the duration of toxin competition (>3.5 mM, 232.46 mg/L NO_3) was highly significant at $p>0.01$ (Figure 3.11), with phosphate significant difference post *P. ferrooxidans* inoculation at day 15 at $p>0.05$ (Figure 3.23). Early phosphate differences can be largely but not exclusively be ascribed to phosphate precipitation in the form of vivianite mineral or sorption, as all phosphate levels began as 3.33 mg/L in standard media, and phosphate determination began after ferrous chloride introduction. Generally speaking, late lag phosphate assimilation of *M. aeruginosa* ranges from ~1/50 to 1/100 of a mg/L PO_4 per day, with 4.88E-9 (mg/L) s^{-1} lag phase for non-toxin strain and 1.46E-8 (mg/L) s^{-1} for the lag phase toxin producing strain as 1-10uM P-PO_4 (Table 3.4). Internalization of phosphate is not

uncommon for cyanobacteria, however the strains of *M. aeruginosa* utilized in this experiment are not known to internalize, however it has shown only to occur in cyanobacteria and many other aquatic bacteria, when P-PO_4 is highly depleted (Hudek et al. 2016); and therefore exponential growth cannot be owed to early internalization or rapid assimilation of pre-saturated, mineralized PO_4 concentrations. Logarithmic phase phosphate assimilation rates increases to 1.57E-8 (mg/L) s^{-1} for the non-toxin strain and 1.88E-8 (mg/L) s^{-1} for the toxin strain, illustrating increased assimilation while under rapid growth as opposed to the late log phase.

4.1.4 Biomineralization and Mineralization

Geochemical saturation indices show a steady likelihood of phosphate to precipitate in the form of unexclusive vivianite $(Fe^{2+})_3(PO_4)_2 \cdot 8H_2O$ due to the presence of ferric iron at t=0 (Figures 3.9, 3.14), followed by Fe (III) – hydroxide and several other iron oxides namely, hematite, goethite and the hydrous sulfate of iron, k-jarosite (Figure 3.16). Further oxidation to metavivianite $(Fe^{2+})_{3-x}(Fe^{3+})_x(PO_4)_2(OH)_x \cdot (8-x)H_2O$ was also observed, with the possibility of masked quantities of ferrostrunzite $Fe^{2+}Fe_2^{3+}(PO_4)_2(OH)_2.(5H_2O.OH)$ produced as well. Microaerophilic oxidation produced secondary minerals of fined grained character (1.0-10.0 um) that are common in biomineralization, with the propensity of Mg^{2+}, Ca^{2+} displacement due to the high concentrations that were used in the experiment. P –phosphate was highly bound ~90%, during the introduction of ferrous iron (molar Fe:P >2.5) (Figure 3.9, 3.14). Due to microaerophilic conditions, incremental neoformation was observed over a twelve day period. Both time zero saturation indices of non-toxin and toxin experiments measured at 3.80 and shifted to 0.44 and 0.55 (mean of triplicate analyte P, N, Fe), respectively (Figures 3.9, 3.14).

Qualitatively, anion concentration dependent green rusts of high inclination to formation (GR-Cl, GR-SO_4) was not observed and was predictably inhibited by rich phosphate conditions during the process of ferrous iron oxidation (Miot et al. 2009). However, little is known regarding the potential biomineralization transformations of saturated vivianite by *P. ferrooxidans sp. MAI-1* under minimal P, including the presence of long term nitrite and ferrous iron transformations, namely the potentiality of amorphous transformations under limited atmosphere (Hansen & Poulsen, 1999; Miot et al. 2009). Future research should address the prospective long term biogeochemical mixed valence metavivianite transformations by *P. ferrooxidans sp. MAI-1*, such as the further oxidation of metavivianite to complete Fe (III) oxidation (Figures 3.9, 3.14) that may result in the formation of ferristrunzite $Fe^{3+}Fe_2^{3+}(PO_4)_2(OH)_2.(5H_2O.OH)$. Hydration however, may have constrained this outcome, and such predictability geochemical software modelling lacks (Frost et al. 2004). Practically speaking, the addition of iron is necessary to provide an electron donor flux for the competitor *P. ferrooxidans*, permitting the competitor to grow and denitrify over long periods of time. Given iron heavily oxidizes at microaerophilic interface, the amount of iron passaging through membrane to the cyanobacteria side was trivial and could not be quanitifed by spectrophotometric methods.

4.1.5 Remarks on the Objectives and Hypotheses

The addition of *P. ferrooxidans* at the early logarithmic growth phase of the cyanobacteria (at day 7) resulted in mechanistic non exclusive nitrogen competition by means of *P. ferrooxidans* denitrification. This is demonstrated by significant total nitrogen loss compared to the control towards both *M. aeruginosa* strains all the way up to day 15 (Figure 3.6, 3.11).

Nitrogen loss due to competition was determined by quantifying total nitrogen in the system over a fifteen day period, and the detection of the nitrate derivative nitrite. The exceedance of molar nitrogen assimilation to phosphorus was five hundred times more, with a total microbial competition difference of ~0.1 mg/L PO_4 indicating that nitrogen was a substantial contributor to the change in cyanobacterial logarithmic growth. Moreover, total average phosphate was significant compared to the control for the toxin producing strain of cyanobacteria, but was not significant for the non toxin producing strain of cyanobacteria. This may suggest that practically speaking, when *M. aeruginosa* is placed under the presence of a novel inorganic competitor such as *P. ferrooxidans*, nitrogen assimilation by the competitor is more effective at diminishing a cyanobacteria bloom as opposed to phosphorus assimilation by this competitor. In both the toxin and non toxin experiments, cyanobacteria demonstrated a significant cell count drop after day seven, and further by ~25% at day 18 when compared to the control experiment. This early cell death phase of the cyanobacteria implies that the introduction of a novel denitrifier such as *P. ferrooxidans*, and can reduce the total logarithmic cell count of an early cyanobacterial bloom, if introduced during the early logarithmic phase (day 7 of cyanobacterial growth). Therefore, the (1) null hypothesis can be rejected, and the introduction of *P. ferrooxidans* did result in competitive exclusion of the early logarithmic cyanobacteria owing to rapid non exclusive denitrification.

4.1.5 A Remediation Strategy of the Future?

In the least, the microbial competition under a microaerophilic interface outlined in this study suggests that fast denitrifying *P. ferrooxidans* can significantly abate a growing toxin to

non-toxin bloom. Environmentally and practically speaking, additions of *P. ferrooxidans* through column diffusion could serve to remediate cyanobacterial blooms under nitrogen enriched environments. The next stage would be to investigate this experiment under a natural environment to determine if any natural boundaries exist. Examples of these natural boundaries include location unique community structures, the presence of heterocystic strains, shifts in natural water temperatures etc. Geologically speaking, NDFe(II)OB such as *P. ferrooxidans* and cyanobacteria such as *M. aeruginosa* have been suspected to largely exist together during the Archean period, and today within deep lake facsimiles such as lake Matano, Kabuno Bay (Lliros et al. 2015; Sabo 2006), and may have played a community role in the formation of Banded Iron Formations during the Neoarchean period (Nutman et al. 2016; Schirrmeister et al. 2015). This dual implication, illustrates the importance of selecting the strain *P. ferrooxidans sp. MAI-1* that was isolated from a Neoarchean lake Matano, for this particular experiment. In the future, community studies should focus on barriers or factors that reinforce or diminish competition to better understand dually the broader environmental and Neoarchean implications. Moreover, under continual electron donor flux, *P. ferrooxidans sp. MAI -1* is a bacterium capable of significantly abating a cyanobacteria bloom, or is a novel method of bioremediating largely phosphorus and nitrogen polluted eutrophied fresh bodies of water.

5. Conclusion

Assessment of *P. ferrooxidans sp. MAI-1* has demonstrated its capacity to exist in a wide variety of diverse environments, owing to its ability to utilize many forms of iron as electron donor (magnetite, mono ferrous sulfide, etc.). The Fe (II) – Fe (III) redox couple is an important

electron supplant for energy in natural environments and is largely mediated by microorganisms under stable oxygen free waters, such as nitrate dependent chemotrophs. In this study, microbial growth competition was investigated by means of chamber diffusion and chemical nutrient quantification, demonstrating that *P. ferrooxidans sp. MAI-1* as rapid denitrifier and iron oxidizer that can significantly abate a toxic cyanobacterial bloom at microaerophilic interface, under both toxin and non-toxin concomitancy, which brings to query the degree of modularity that exist within denitrifying communities. Nitrogen removal by way of reduction competition has shown to be significant, which reaffirms the position held by Levy 2017. Remediation protocols should focus on N removal under early logarithmic phases of cyanobacteria as a mitigation strategy for toxic blooms. Furthermore, this study has revealed that the presence of carbon and iron as electron donor may serve as restoring balance of highly contaminated or nutrient rich water systems, commonly found within iron poor but inorganically polluted environments, by promoting the synthesis of vivianite in the case of uncontrolled practical applications. Moreover, it is know that low phosphate release in anoxic environments is linked to iron poor sediments, and in these cases direct ferrous iron additions may be environmentally viable (Orihel et al. 2015). As previously stated, *M. aeruginosa* growth as cell counts, is abated under an unexclusive N-N dichotomy of rapid nitrogen depletion by the competitor *P. ferrooxidans*. This reaffirms the practical plausibility of competitive exclusion and likely not niche differentiation. Little is known regarding the interaction of dominant *M. aeruginosa* with respect to natural community dynamics of other N-P utilizing organisms and future actualistic community research is warranted, but if it is anything that we can learn from contemporary research, it is that microorganisms do not conform to traditional boundaries. Further studies of *P. ferrooxidans sp.MAI-1* interaction with microcystinsshould focus on building effective methods and detailing

the affects of toxin exposure. Further investigation should focus on replicating natural communities in hopes of better understanding natural competition barriers and the potential to existing relationships there within.

6. References

Azevedo SM., Carmichael W.W., Jochimsen E.M., Rinehart K.L., Lau S., Shaw G.R. and Eaglesham G.K. (2002). Human intoxication by microcystins during renal dialysis treatment in Caruaru-Brazil. *Toxicology* 181–182: 441-446.

Berman-Frank, I., Lundgren, P. and Falkowski, P. (2003). Nitrogen fixation and photosynthetic oxygen evolution in cyanobacteria. *Res. Microbiol.* 154, 157–164.

Cabello, P., Roldan, M. D. and Moreno-Vivian C. (2004). Nitrate reduction and the nitrogen cycle in archaea. *Microbiology* 150: 3527–3544.

Canfield, D.E. (1989). Reactive iron in marine sediments. *Geochim Cosmochim Acta* 53: 619–632.

Canfield, D. E. and Thamdrup, B. (2005). Aquatic Geomicrobiology, Elsevier Academic Press.

Caranto J. D. and Lancaster, K. M. (2017). Nitric oxide is an obligate bacterial nitrification intermediate produced by hydroxylamine oxidoreductase. *PNAS* 114: 8217–8222.

Cecchini S. and Caputo A. R. (2012). A Direct Spectrophotometric Assay for Evaluating Nitrate-Nitrogen in Intensive Aquaculture Systems. *The Israeli Journal of Aquaculture – Bamidgeh* 64: 2-6.

Chaffin J. D., Bridgeman T. B. and Bade D. L. (2013). Nitrogen constrains the growth of late summer cyanobacterial blooms in Lake Erie. *Adv. Microbiol.* 3: 16-26.

Chen W., Tong H. and Liu H. (2012). Effects of nitrate on nitrite toxicity to *Microcystis aeruginosa*. *Mar. Pollut. Bull*. 4:1106-1111.

Chen L. and Xie P. (2016). Mechanisms of Microcystin-induced Cytotoxicity and Apoptosis.

Mini Rev. Med. Chem. 16: 1018-1031.

Cheng, Y. S., Yue Z., Irvin M. C., Kirkpatrick B. and Backer L. C. (2007). Characterization of Aerosols Containing Microcystin. *Mar. Drugs* 5:136-150.

Cornell, R. M. and Schwertmann, U. (2003). The Iron Oxides: Structure, properties, reactions, occurrences, and uses. Wiley-VCH, Weinheim.

Dawson R.M (1998). The toxicology of microcystins. *Toxicon.* 36: 953-962.

Dijkstra N., Slomp C. P. and Behrends T. (2016). Vivianite is a key sink for phosphorus in sediments of the Landsort Deep, an intermittently anoxic deep basin in the Baltic Sea. *Chem. Geol.* 438: 58-72.

Dodd, M.S., Papineau, D., Grenne, T., Slack, J.F., Rittner, M., Pirajno, F., O'Neil, J. and Little, C.T.S. (2017). Evidence for early life in Earth's oldest hydrothermal vent precipitates. *Nature* 543:60-64.

Donelon M. A., Drennan W. M., Saltzman E. S. and Wanninkhof R. (Eds.) (2002). Gas Transfers at Water Surfaces. The American Geophysical Union., vol. 127, DOI:10.1029/GM127

Eady, R. R. (1996). Structure-function relationships of alternative nitrogenases. *Chem. Rev.* 96: 3013–3030.

Erisman, J. W., Sutton, M. A., Galloway, J., Klimont, Z. and Winiwarter, W. (2008). How a century of ammonia synthesis changed the world. *Nat. Geosci.* 1: 636–639.

Ernst A., Manfred D., Herman, M. J., Ute I. and Wollenzien A. (2005). Nitrate and Phosphate Affect Cultivability of Cyanobacteria from Environments with Low Nutrient Levels. *Microb. Ecol.* 71: 3379-3383.

Emerson, D. (2016). The Irony of Iron - Biogenic Iron Oxides as an Iron Source to the Ocean. *Front. Microbiol.* 6:1502-1514.

Emerson, D., Weiss, J. V. and Megonigal, J. P. (1999). Ironoxidizingbacteria are associated with ferric hydroxideprecipitates (Fe-plaque) on the roots of wetlandplants. *Appl. Environ. Microbiol.* 65:2758–2761.

.

Fang, F. C. (2004). Antimicrobial reactive oxygen and nitrogen species: concepts and controversies. *Nat. Rev. Microbiol***.** 2: 820–832.

Frost, R. L.,Weier, M. L. and Lyon, W. (2004). Metavivianite an intermediate mineral phase between vivianite, and ferro/ferristrunzite: a Ra-man spectroscopic study. *Neues Jahrbuch fuer Mineralogie Monatshefte* 5: 228-240.

Galloway, J. N., Townsend A. R., Erisman J. W., Bekunda M., Cai Z., Freney J. R. and Luiz A. (2008). Transformation of the nitrogen cycle: recent trends, questions, and potential solutions. *Science* 320: 889–892.

Gobler C.J., Burkholder J.M., Davis T.W., Harke M.J., Johengen T., Stow C.A. and Van de Waal D.B. (2016). The dual role of nitrogen supply in controlling the growth and toxicity of cyanobacterial blooms. *Harmful Algae* 54: 87-97.

Gruber, N (2008). The marine nitrogen cycle: overview and challenges. In: Nitrogen in the Marine Environment (2nd Edition), Academic Press, Editors: Capone D.G., Bronk D.A., Mulholland M.R. and Carpenter, E.J., pp.1-50

Gruber, N. and Galloway, J. N. (2008). An Earth-system perspective of the global nitrogen cycle. *Nature* 451: 293–296.

Hansen, H.C.B. and Poulsen, IF. (1999) Interaction of synthetic sulphate "green rust" with phosphate and the crystallization of vivianite. *Clays and Clay Minerals* 47: 312-318.

Harke M., Steffen M.M., Gobler C.J., Otten T.G., Wilhelm S.W., Wood S.A. and Paerl H.W. (2016). A review of the global ecology, genomics and biogeography of the toxic cyanobacterium, *Microcystis* spp. *Harmful Algae* 54: 4-20.

Henry T. (2014). Lake Erie, South Florida Algae Crises Share Common Toxins and Causes. *Toledo Blade.* Local section, online edition (https://www.toledoblade.com/local/2016/07/24/Lake-Erie-S-Florida-algae-crises-share-common-toxins-and-causes.html).

Hooper, A. B., Vannelli, T., Bergmann, D. J. and Arciero, D. (1997). M. Enzymology of the oxidation of ammonia to nitrite by bacteria. *Antonie Leeuwenhoek* 71: 59–67.

Hudek L., Premachandra D., Webster W. A. J., and Bräu L. (2016). Role of Phosphate Transport System Component PstB1 in Phosphate Internalization by Nostoc punctiforme. *Appl. Environ. Microbiol.* 82:6344-6356.

Ilberta, M. and Bonnefoy,V. (2013). Insight into the evolution of the iron oxidation pathways. *Biochimica et Biophysica Acta (BBA) – Bioenergetics* 1827: 161-175.

Kendelewicz T., Kaya S., Newberg J. T., Bluhm H., Mulakaluri N., Moritz W., Scheffler M., Nilsson A., Pentcheva R. and Brown G. E. Jr. (2013). X-ray Photoemission and Density Functional Theory Study of the Interaction of Water Vapor with the Fe3O4 (001) Surface at Near-Ambient Conditions. *J. Phys. Chem. C*.117: 2719–2730.

Kopf S. H., Henny C. and Newman D. K. (2013). Ligand-Enhanced Abiotic Iron Oxidation and the Effects of Chemical versus Biological Iron Cycling in Anoxic Environments. *Environ. Sci. Technol.* 47: 2602–2611.

Kuypers M. M., Hannah M., Marchant K. and Kartal B. (2018). The microbial nitrogen-cycling network. Microbial biogemochemistry Reviews. *Nature Reviews* 16: 263-270.

Lam P., Lavik G., Jensen M.M., van de Vossenberg J., Schmid M., Woebken D., Gutiérrez D., Amann R., Jetten M.S. and Kuypers M.M. (2009). Revising the nitrogen cycle in the Peruvian oxygen minimum zone. *PNAS* 106: 4752–4757.

Lam, P. and Kuypers M. M. (2011). Microbial Nitrogen Cycling Processes in Oxygen Minimum Zones. *Ann. Rev. Mar. Sci.* 3: 317–345.

Levy S. (2017). *Microcystis* Rising: Why Phosphorus Reduction Isn't Enough to Stop CyanoHABs. *Environ Health Perspect.* 125: A34–A39.

Lliros M., García–Armisen T., Darchambeau F. , Morana C. , Triadó–Margarit X. , Inceoğlu Ö. , Borrego C. M. , Bouillon S., Servais P., Borges A. V. , Descy J. , Canfield Don E. and Crowe S. A. (2015). Pelagic photoferrotrophy and iron cycling in a modern ferruginous basin. *Scientific Reports 5:* 13803-13812.

Lovley, D. R., Coates, J. D., Blunt-Harris, E. L., Phillips, E. J. P. and Woodward, J. C (1996). Humic substances as electron acceptors for microbial respiration. *Nature* 382: 445–448

Maalcke W. J., Dietl A., Marritt S.J., Butt J.N., Jetten M.S., Keltjens J.T., Barends T.R. and Kartal B. (2014). Structural basis of biological NO generation by octaheme oxidoreductases. *J. Biol. Chem.* 289: 1228–1242.

Mendiboure, A. and Schöllhorn, A. (1986). Formation and anion exchange reactions of layered transition metal hydroxides [Nii.xMx](OH)2(C03)x/2(H20)z (M = Fe, Co). *Revue de Chimie Minérale* 23: 819-827.

Michalak A., Anderson E.J., Beletsky D., Boland S., Bosch N.S., Bridgeman T.B., Chaffin J.D., Cho K., Confesor R., Daloglu I., Depinto J.V., Evans M.A., Fahnenstiel G.L., He L., Ho J.C., Jenkins L., Johengen T.H., Kuo K.C., Laporte E., Liu X., McWilliams M.R., Moore M.R.,

Miot J., Benzerara K., Morin G., Bernard S., Beyssac O., Larquet E., Kappler A. and Guyot F. (2009). Transformation of vivianite by anaerobic nitrate-reducing iron-oxidizing bacteria. *Geobiology* 7: 373–384.

Mitsch W.J., Day J. W., Zhang L. and Lane. R. R. (2005). Nitrate-nitrogen retention in wetlands in the Mississippi River basin. *Ecol. Eng.* 24: 267-278.

Moore J. K. and O. Braucher (2008). Sedimentary and mineral dust sources of dissolved iron to the world ocean. *Biogeosciences* 5: 631-656.

Moreno-Vivian C., Martinez-Luque P., Blasco M. R. and Castillo, F. (1999). Prokaryotic nitrate reduction:molecular properties and functional distinction among bacterial nitrate reductases. *J. Bacteriol.* 181: 6573–6584.

Newton, R. J., Jones, S. E., Eiler, A., McMahon, K. D., Bertilsson S.(2011). A Guide to the Natural History of Fresh Water Lake Bacteria. *Microbiology and Molecular Biology Reviews*75: 14-49.

Nriagu, J.O. and Dell, CI. (1974) Diagenetic formation of iron phosphates in recent lake sediments. *Am. Mineralogist* 59: 934-946.

Nutman, A.P., Bennett, V.C., Friend, C.R.L., Van Kranendonk, M.J., Chivas, A.R. (2016). Rapid emergence of life shown by discovery of 3,700-million-year-old microbial structures. *Nature* 537:535-538.

Orihel Di. M., Schindler D. W., Ballard N. C., Graham M. D., O'Connell D. W., Wilson L. R. and Vinebrooke R. D. (2015). The “nutrient pump:” Iron-poor sediments fuel low nitrogen-to-phosphorus ratios and cyanobacterial blooms in polymictic lakes. *Limnol. Oceanogr.* 60: 856-871.

Pérez-Guzmán, L., Bogner, K. R. and Lower, B. H. (2010) Earth's Ferrous Wheel. *Nature Education Knowledge* 3:32-34

Preisler A., de Beer D., Lichtschlag A., Lavik G., Boetius A. and, Jørgensen B.B. (2007). Biological and chemical sulfide oxidation in a Beggiatoa inhabited marine sediment. *ISME J.* 1: 341–353.

Rabalais N. N. (2002). Nitrogen in Aquatic Ecosystems. *Royal Swedish Academy of Sciences Ambio* 31: 102-112.

Raiswell R., and Canfield D. E. (2012). The Iron Biogeochemical Cycle Past and Present. *Geochemical Perspectives* 1: 1-2.

Robertson, E. K., Roberts, K. L., Burdorf, L. D. W., Cook, P. and Thamdrup, B (2016). Dissimilatory nitrate reduction to ammonium coupled to Fe(II) oxidation in sediments of a periodically hypoxic estuary. *Limnol. Oceanogr.* 61: 365–381.

Rothe M., Kleeberg A. and Hupfer M. (2016). The occurrence, identification and environmental relevance of vivianite in waterlogged soils and aquatic sediments. *Earth-Science Reviews* 158: 51–64.

Sabo, E. (2006). Characterization of the pelagic plankton assemblage of Lake Matano and determination of factors regulating primaryand secondary production dynamics,. *Electronic Theses and Dissertations, University of Windsor* 6942.

Saraiva, L. M., Vicente, J. B. and Teixeira, M. (2004). The role of the flavodiiron proteins in microbial nitric oxide detoxification. *Adv. Microb. Physiol.* 49: 77–129.

Schindler D. W. (1997). Evolution of phosphorus limitation in lakes. *Science* 195: 260-262.

Schindler, D. W., Hecky R. E., Findlay D. L., Stainton M. P., Parker B. R., Paterson M. J., Beaty K. G., Lyng M.. and Kasian S. E. M. (2008). Eutrophication of lakes cannot be controlled by reducing nitrogen input: Results of a 37-year whole-ecosystem experiment. *PNAS* 105: 11254-11258.

Schirrmeister B., Gugger M. and, Donoghue P.C. (2015). Cyanobacteria and the great oxidation event: evidence from genes and fossils. *Palaeontology* 58: 769-785.

Schnetger B. and Lehners C. (2014). Determination of nitrate plus nitrite in small volume marine water samples using vanadium(III)chloride as a reduction agent. *Mar. Chem.* 160: 91–98.

Smith. M. T, Smith R. L. and Waters I. (2012). Elements of Ecology, Pearson Education Inc.

Steffen M.M., Belisle B. S., Watson S. B., Boyer G. L. and Wilhelm S. W. (2014). Status, causes and controls of cyanobacterial blooms in Lake Erie. *J. Great Lakes Res.* 40: 215-225.

Stein, L. Y. and Klotz, M. G (2016). The nitrogen cycle. *Curr. Biol*. 26, R94–R98.
Stookey, Lawrence L. (1970). Ferrozine---a new spectrophotometric reagent for iron. *Anal. Chem.* 42: 779–781.

Straub K. L., Schonhuber W. A., Buchholz-Cleven B. E. E. and Schink B. (2004). Diversity of Ferrous Iron-Oxidizing, Nitrate-Reducing Bacteria and their Involvement in Oxygen-Independent Iron Cycling. *Geomicrobiol. J.* 21: 371–378.

Straub, K. L., Benz M. and Schink B. (2001). Iron metabolism in anoxic environments at near neutral pH. *FEMS Microbiol. Ecol.* 34: 181-186.

Straub KL.., Benz M., Schink B. and Widdel F. (1996). Anaerobic, nitrate-dependent microbial oxidation of ferrous iron. *Appl. Environ. Microbiol.* 62:1458-1460.

Strumm, W. and Morgan, J. J. (1996). Aquatic chemistry: Chemical equilibria and rates in natural waters. John Wiley and Sons, New York.

Towns, T. G. (1986). Determination of aqueous phosphate by ascorbic acid reduction of phosphomolybdic acid. *Anal. Chem.* 58: 223–229.

Utkilen H. and Gjolme N. (1992). Toxin Production by *Microcystis aeruginosa* as a Function of Light in Continuous Cultures and Its Ecological Significance. *Appl. Environ. Microbiol.* 58: 1321-1325.

Vitousek, P. M. and Howarth, R. W (1991). Nitrogen limitation on land and in the sea: How can it occur? *Biogeochemistry* 13: 87–115.

Walsby A.E., Hayes P.K., Boje R. and Stal L. J. (1997). The selective advantage of buoyancy provided by gas vesicles for planktonic cyanobacteria in the Baltic Sea. *New Phytol.* 136: 407–417.

Wasmund K., Mußmann M. and Loy A. (2017). The life sulfuric: microbial ecology of sulfur cycling in marine sediments. *Environmental Microbiology Reports* 9: 323–344.

Watson S.B., Miller C., Arhonditsis G., Boyer G.L., Carmichael W., Charlton M.N., Confesor R., Depew D.C., Höök T.O., Ludsin S.A., Matisoff G., McElmurry S.P., Murray M.W., Richards P. R., Rao Y.R., Steffen M.M. and Wilhelm S.W. (2016). The re-eutrophication of Lake Erie: harmful algal blooms and hypoxia. *Harmful Algae* 56: 44-66.

Weber K. A., Achenbach L. A. and Coates J. D. (2006). Microorganisms pumping iron: anaerobic microbial iron oxidation and reduction. *Nature* 4: 752-764.

Zumft, W. G (1997). Cell biology and molecular basis of denitrification. *Microbiol. Mol. Biol. Rev.* 61: 533–616.

Appendix (supplementary material)

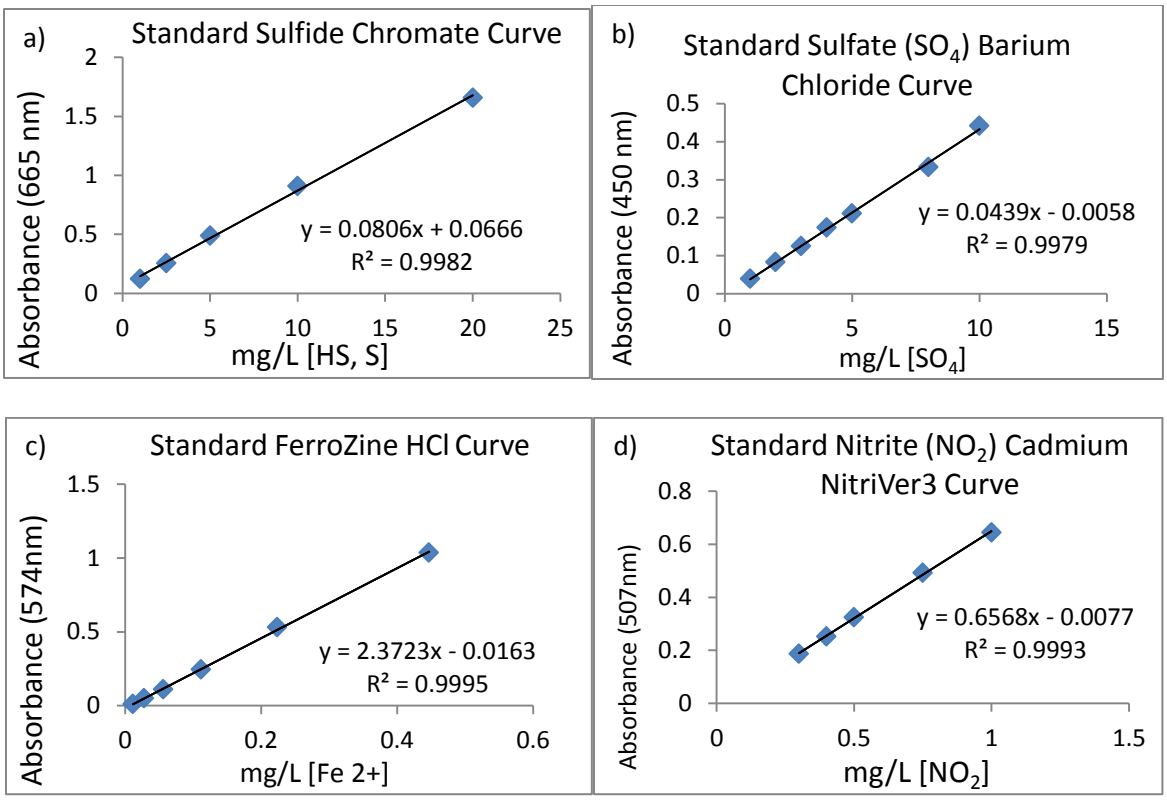

Figure S.1 – Standard determination curves using spectrophotometric reagents, a) standard sulfide curve using Cline's and Chromate, b) standard sulfate curve using barium chloride, c) standard iron curve using HCl and FerroZine, d) standard nitrite curve using HACH cadmium Nitriver 3.

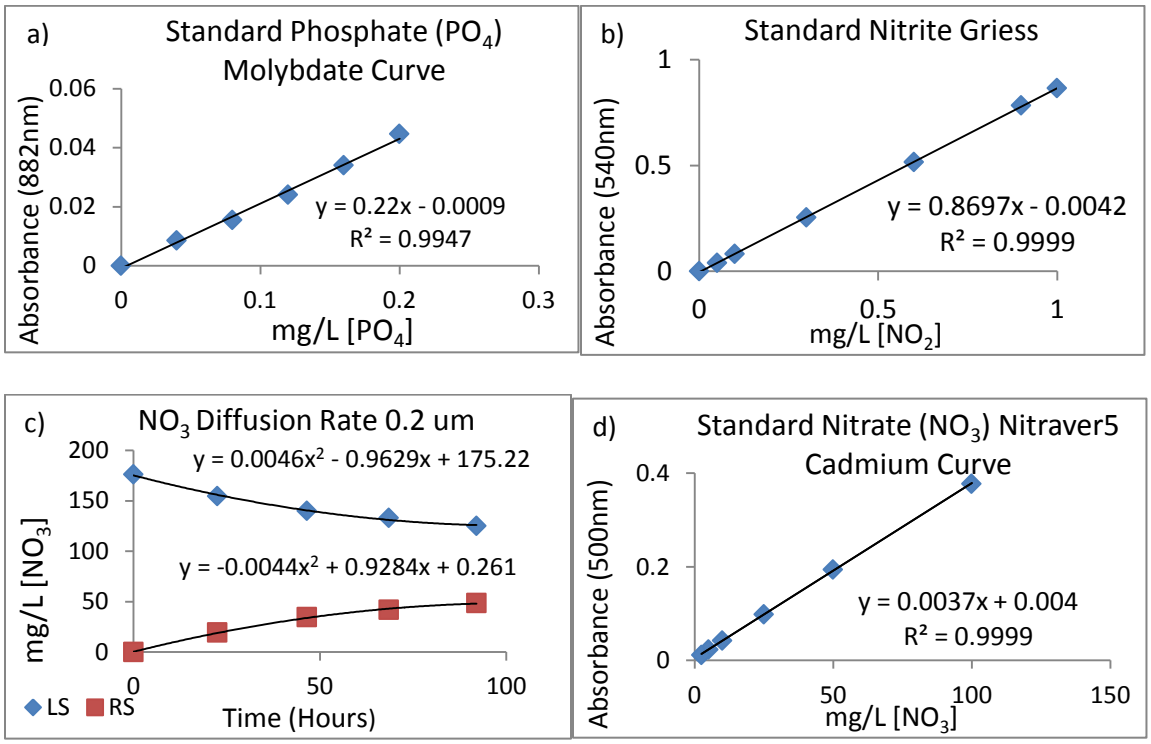

Figure S.2 – Standard determination curves using spectrophotometric reagents and a diffusion rate, a) standard phosphate curve using molybdate and ascorbic acid, b) standard nitrite curve using Griess reagent, c) diffusion rate of nitrate under 0.20 um Millipore filter paper at 182 mg/L (6 mM), standard nitrate curve using HACH cadmium Nitraver 5.

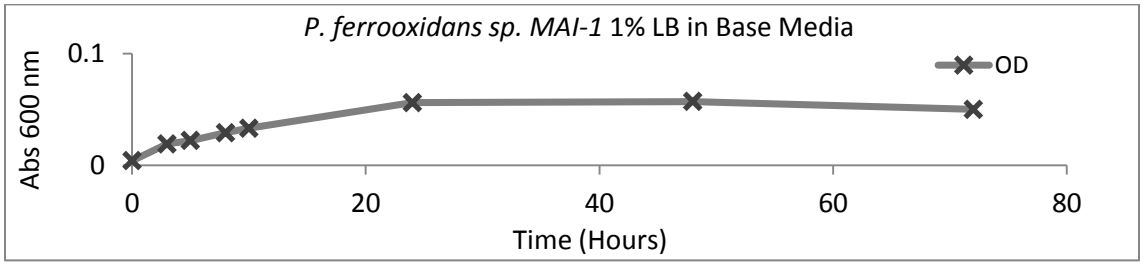

Figure S.3 – *P. ferrooxidans* growth as optical density in 1% lysogeny broth composition and denitrifying media, showing a short logarithmic period (< 20 hours). In gray optical density at 600 nm where error bars represent σ (standard deviation) of mean of triplicate. Error bars too small to be displayed are hidden behind symbol.

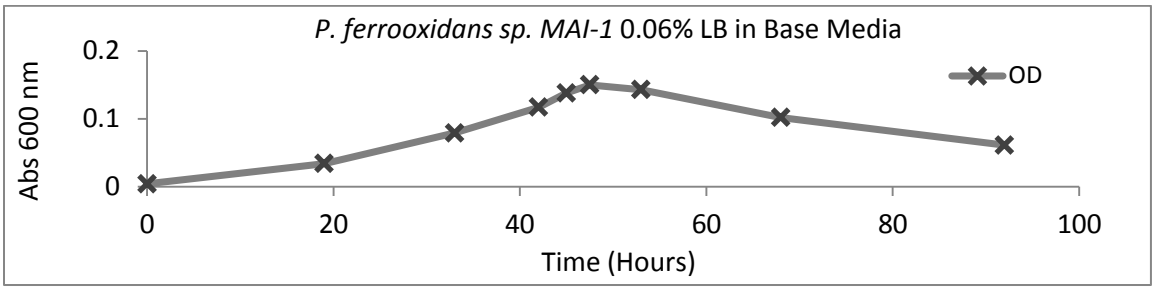

Figure S.4 – *P. ferrooxidans* growth as optical density in 0.06% lysogeny broth composition and denitrifying media, showing an increased logarithmic period (> 40 hours). In gray optical density at 600 nm, where error bars represent σ (standard deviation) of mean of triplicate. Error bars too small to be displayed are hidden behind symbol.

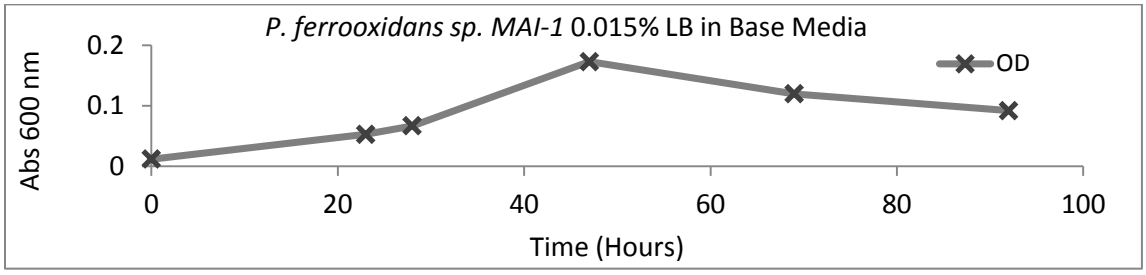

Figure S.5 – *P. ferrooxidans* as optical density in 0.015% lysogeny broth composition and denitrifying media, showing an increased logarithmic period with higher density by acclimation (> 40 hours). In gray optical density at 600 nm, where error bars represent σ (standard deviation) of mean of triplicate. Error bars too small to be displayed are hidden behind symbol.